UNIVERSITY OF RIJEKA

FACULTY OF MEDICINE

Mia Krapić

INTERACTIONS BETWEEN ADIPOSE TISSUE AND THE
IMMUNE SYSTEM IN THE CONTEXT OF INFECTION

Doctoral thesis

Rijeka, 2023

UNIVERSITY OF RIJEKA

FACULTY OF MEDICINE

Mia Krapić

INTERACTIONS BETWEEN ADIPOSE TISSUE AND THE
IMMUNE SYSTEM IN THE CONTEXT OF INFECTION

Doctoral thesis

Mentor: dr. sc. Felix M.Wensveen, PhD

Co-mentor: dr. sc. Tamara Turk Wensveen, MD, PhD

Rijeka, 2023

Mentor rada: izv. prof. dr. sc. Felix M. Wensveen, dip. biol.

Ko-mentor rada: izv. prof. dr. sc. Tamara Turk Wensveen, dr. med.

Doktorska disertacija obranjena je dana _____ u/na _____

_____, pred povjerenstvom u sastavu:

1. _____ (titula, ime i prezime)

2. _____ (titula, ime i prezime)

3. _____ (titula, ime i prezime)

4. _____ (titula, ime i prezime)

5. _____ (titula, ime i prezime)

Rad ima _____ listova.

UDK: _____ (UDK broj dodjeljuje Knjižnica Medicinskog fakulteta u Rijeci)

PREDGOVOR

SUMMARY

Objectives: In context of metabolic disease, adipocytes were shown to pathologically interact with the immune system. When becoming obese, these cells drive inflammation in adipose tissue, which alters local and systemic regulation of metabolism. However, how adipocytes interact with immune cells in context of viral infection is largely unknown. Our objective was to investigate the impact of virus-induced activation of the immune system on adipose tissue metabolism and the underlying benefit of these changes to the organism.

Materials and methods: Mice were infected with murine cytomegalovirus (mCMV) as a model of human infection. To determine the impact of mCMV infection on adipose tissue physiology, density of visceral adipose tissue (VAT) was measured by x-ray and adipocyte size by histology. To investigate the impact of immune-adipocyte interactions in vitro, we made use of the 3T3-L1 model. Lipid content was quantified histologically with Oil red O staining or by flow cytometry after BODIPY staining, upon treatment with different cytokines. The impact of IFNγ on key metabolic genes was determined by micro-array and confirmed by RT-PCR analysis. The role of specific immune cells, cytokines and stress receptors was determined through antibody-mediated neutralization or by using genetic mouse models. Mass spectrometry was used to determine the lipidomic profile of mouse plasma after infection. Finally, to determine the impact of lipids on the immune system, we made use of the A20 B cell line. Cells were characterized with flow cytometry and Seahorse analysis upon treatment with fatty acids.

Results: Upon mCMV infection, VAT transiently decreases in size and density, with a maximum effect after 3 days. Adipocytes increase expression of ligands for the activating NK cell receptor NCR1. NK cells are activated through NCR1 and produce high amounts of IFNγ. This cytokine directly targets adipocytes and downregulates the key transcription factor PPARγ and its target genes. The result is adipocyte size reduction, and release of fatty acids such as oleic acid into the bloodstream. This effect was prevented if mice were deficient for NCR1, IFNγ, or the IFNγ receptor on adipocytes and if NK cells were depleted using antibodies. Serum levels of oleic acid were increased in particular, and this fatty acid promotes ATP production and increases activation of A20 B cells in vitro. Importantly, in animals deficient for IFNγ, B cell activation was significantly reduced.

Conclusion: Infection causes activation of NK cells in VAT, which induces lipid release by adipocytes following direct stimulation by IFNγ. The increase in systemic lipids promotes the activation of B cells. Our findings provide a physiological explanation for the interactions between the immune system and adipose tissue in the context of inflammation. A better understanding of these mechanisms of metabolic regulation by the immune system can be highly beneficial for comprehension and treatment of infection-induced complications in the context of the metabolic disease.

Key words: Adipose tissue; Immune system; Infections; Metabolism; PPAR gamma.

SAŽETAK

Ciljevi: U kontekstu metaboličkih bolesti, adipociti patološki među-djeluju s imunim sustavom. Kod pretilosti, ove stanice potiču upalu u masnom tkivu, koje djeluje na lokalnu i sistemsku regulaciju metabolizma. Kako adipociti među-djeluju s imunim stanicama u kontekstu virusne infekcije je još uvijek nepoznato. Naš je cilj bio istražiti utjecaj virusom aktiviranog imunog sustava na metabolizam masnog tkiva i prednosti ovih promjena za organizam.

Materijali i metode: Miševi su inficirani s mišjim citomegalovirusom (mCMV) kao modelom infekcije u ljudi. Kako bi odredili utjecaj mCMV infekcije na fiziologiju masnog tkiva, gustoća visceralnog masnog tkiva je određena rendgenom, a veličina adipocita histologijom. Utjecaj među-djelovanja adipocita i imunih stanica *in vitro* odredili smo 3T3-L1 staničnim modelom. Sadržaj lipida kvantificiran je histološki s Oil red O bojenjem ili protočnom citometrijom BODIPY bojenjem, nakon tretmana s različitim citokinima. Utjecaj IFNγ na ključne metaboličke gene bio je mjeren DNA-čip metodom i potvrđen metodom lančane reakcije polimerazom u stvarnom vremenu. Uloga specifičnih imunih stanica, citokina i receptora određena je neutralizacijom s anti-tijelima ili genetičkim mišjim modelima. Masena spektrometrija korištena je za analizu lipida u mišjoj krvnoj plazmi nakon infekcije. Na kraju, kako bi odredili učinak lipida na imuni sustav, koristili smo A20 staničnu liniju. Stanice su analizirane s protočnom citometrijom i Seahorse analizom nakon tretmana s masnim kiselinama.

Rezultati: Nakon mCMV infekcije, visceralno masno tkivo prolazno smanjuje veličinu i gustoću, a maksimalni učinak vidljiv je 3. dan. Adipociti povećavaju ispoljavanje liganada za aktivirajući receptor NK stanica NCR1. NK stanice se aktiviraju pomoću NCR1 i proizvode velike količine IFNγ. Ovaj citokin direktno cilja adipocite i smanjuje ispoljavanje ključnog transkripcijskog faktora PPARγ te gena pod njegovim utjecajem. Rezultat je smanjenje veličine adipocita i otpuštanje masnih kiselina poput oleinske kiseline u krvotok. Ovaj učinak spriječen je kod miševa kojima nedostaje NCR1, IFNγ, ili IFNγ receptor na adipocitima, te ako su NK stanice uklonjene anti-tijelima. Razine oleinske kiseline u serumu bile su značajno povećane, a ova masna kiselina potiče proizvodnju ATP-a i povećava aktivaciju A20 B stanica *in vitro*. Kod životinja kojima nedostaje IFNγ, aktivacija B stanica bila je značajno smanjena.

Zaključak: Infekcija uzrokuje aktivaciju NK stanica u visceralnom masnom tkivu, što potiče otpuštanje lipida iz adipocita nakon direktnog učinka IFNγ. Porast sistemske razine lipida potiče

aktivaciju B stanica. Naši rezultati objašnjavaju fiziološki utjecaj među-djelovanja imunog sustava i masnog tkiva u kontekstu upale. Bolje razumijevanje mehanizama metaboličke regulacije pomoću imunog sustava može biti važno za razumijevanje i tretiranje komplikacija uzrokovanih infekcijom u kontekstu metaboličkih bolesti.

Ključne riječi: Imuni sustav; Infekcije; Masno tkivo; Metabolizam; PPAR gamma.

TABLE OF CONTENTS

1. INTRODUCTION AND LITERATURE REVIEW

1.1 The immune system modulates systemic metabolism in infection.

An important defense mechanism to combat pathogens such as viruses is the development of changes in systemic metabolism, which manifest as sickness behavior. Sickness behavior is an integrated part of the immunological cascade that follows upon pathogen encounter [1]. First, innate immune cells become activated within minutes after a virus enters the organism and infects our cells. These cells migrate to the site of infection where they engage cytotoxic mechanisms to eliminate infected cells. In addition, they secrete a plethora of cytokines to protect the spread of the virus to other cells and induce an adaptive immune response, which reaches full strength within days after the infection [2, 3]. The response to a pathogen is not restricted to changes in immune cells. The activated immune system mediates a number of systemic adaptations, which are perceived as symptoms of sickness such as increased body temperature, loss of appetite, nausea, and fatigue [2]. After a few days, when the infection is cleared, the immune system returns to a less activated state and these symptoms dissipate until a new infection occurs. Whereas sickness behavior is one of the best-known aspects of immune activation in context of infection, the mechanisms by which it is induced and the reasons for its development are not completely clear.

Several immunological mediators were shown to be important for the induction of sickness behavior and these frequently target central regulators of systemic homeostasis. It is known that several pro-inflammatory cytokines can affect the hypothalamus, which then regulates systemic metabolism. For example, IL-6, TNF, or IL-1β can stimulate the hypothalamus to produce prostaglandins that bind to EP3R receptors on neurons. This leads to the activation of the medulla of the adrenal gland and production of norepinephrine [4]. Consequently, processes such as shivering and vasoconstriction occur together with thermogenic events in brown adipose tissue [3, 5-7]. The benefits of fever for the immune response against viral infection have been well documented. It has been shown that fever can be beneficial for the migration and adhesion of lymphocytes into the draining lymph nodes through the T-cell thermal sensory pathway [8]. In addition, elevated body temperature can increase the cytotoxicity and migratory ability of NK cells [5].

Another manifestation of sickness behavior is fatigue which typically lasts days, but can persist for months after the infection is cleared [9]. Pro-inflammatory cytokines produced during infection can cause the feeling of being tired by modifying metabolic pathways through the hypothalamic-pituitary-adrenal endocrine axis. Cytokines stimulate the hypothalamus to produce corticotropin-releasing hormone, which induces adrenocorticotropic hormone (ACTH) secretion by the anterior pituitary gland. This in turn, promotes the release of cortisol, and other adrenocortical hormones by the adrenal gland, which disrupts nutrient homeostasis in tissues such as liver, muscle and adipose tissue. In humans, intravenous injection of TNF, IL-1β, and IL-6 induces fatigue while inhibition of TNF signaling prevents the development of this symptom [3, 10]. In addition, cytokines such as type I interferons can directly stimulate the central nervous system (CNS) and mediate fatigue through neuropsychiatric effects [11]. The immune system can mediate systemic metabolic changes not only through the CNS and endocrine system but also through their direct impact on organs. The cytokine IFNγ induces insulin resistance in the muscle, resulting in reduced glucose uptake and reduced metabolic capacity of myocytes, resulting in muscle fatigue [12]. Therefore, the development of fatigue is a consequence of the activation of the immune system.

Finally, a very important sickness behavior is the loss of appetite, also known as anorexia. Although our immune system puts a steep drain on nutrients for its increased energetic requirements following activation for proliferation and protein synthesis, we reduce our food intake when we feel sick. The reason for this paradox is largely unknown. Systemic administration of cytokines, such as TNF and IL-18 causes anorexia by directly targeting receptors in the CNS [13, 14]. As a result, instead of using external sources of energy, sickness promotes the utilization of alternative, internal nutrient sources. For example, free fatty acids are released from adipose tissue and are used as a source of energy in the liver, which can lead to weight loss [5]. However, why the antiviral response would benefit from a systemic change in metabolism is largely unknown.

In summary, infection-induced immune system activation and cytokine production can cause systemic metabolic changes, which manifest as sickness behavior (Figure 1). However, much remains unknown about how specific aspects of sickness behavior are induced and how they benefit the anti-viral response.
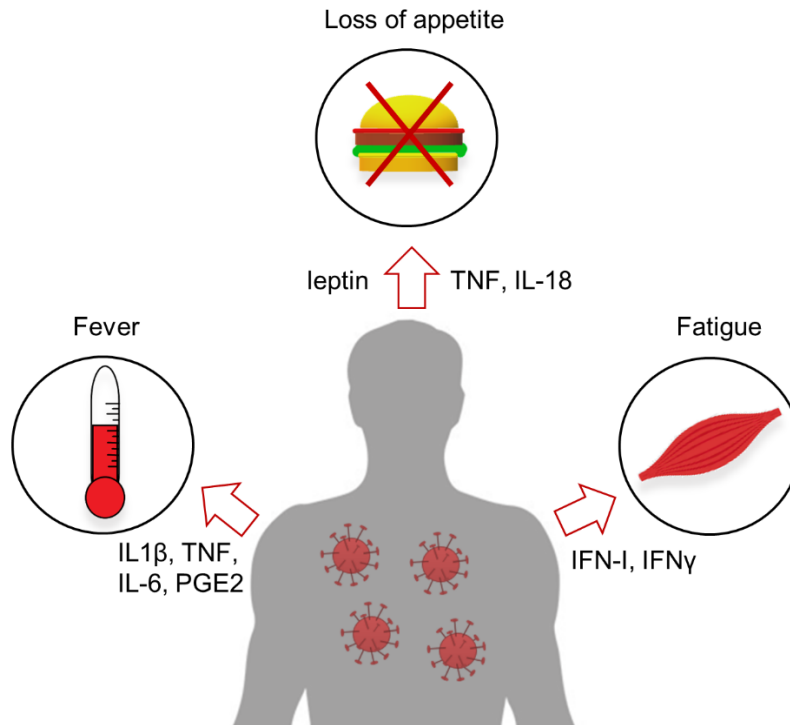
Figure 1. Immune system activation modulates systemic metabolism during viral infection, which manifests as sickness behavior. Fever can be induced by TNF and IL-6. These cytokines, stimulate the brain endothelium to promote the release of prostaglandin E2 (PGE2), which targets the thermoregulatory center in the CNS. Appetite loss is a consequence of TNF and IL-18, which promote leptin production and suppress appetite. Fatigue is induced by type I IFNs and IFNγ which target muscle cells and inhibit nutrient uptake.

1.2. Nutrient requirements of immune system in steady state and activation

The metabolism of immune cells, and thereby the nutrients that they require, is highly dependent on their activation state. Oxidative phosphorylation is used as the preferential means to fulfill energetic needs by resting immune cells such as naïve and memory T cells, M2 macrophages and dendritic cells [15-18]. Upon activation, proliferation, and acquisition of effector functions, these cells undergo drastic metabolic changes. Activated immune cells, in contrast, mostly use glycolysis for adenosine triphosphate (ATP) production and increase their consumption of high-energy nutrients, such as glucose and glutamine. In the absence of glutamine, activated T cells were shown to have a decreased ability to proliferate and produce cytokines [19]. In addition, glucose deprivation reduces the production of IFNγ, perforin, granzyme, and the proliferation of activated NK and T cells [20].

For this reason, the activated immune system puts a major drain on systemic resources. Following infection, up to 30% of all nutrients in the body can be directed towards the activated immune system [18, 21]. Part of the systemic metabolic changes induced upon infection is therefore thought to accommodate immune cell nutrient consumption. For example, concentrations of the short-chain fatty acid acetate increase in the serum following infection. In mice, acetate accumulates in the blood during acute bacterial infection, which is beneficial for memory CD8+ T cell activation. The uptake of acetate by memory CD8+ T cells mediates acetylation of one of the key enzymes important for glycolysis and therefore improves the memory response [22].

On the other hand, recent studies have shown that instead of glycolysis, activated immune cells, such as B cells, preferentially use oxidative phosphorylation in germinal centers. Germinal centers are sites of B lymphocyte proliferation, differentiation and somatic hypermutation [23] and therefore have a high energy demand. To fulfill this, they use free fatty acids as their primary energy source. The inhibition of fatty acid oxidation reduces germinal center formation in mice [24]. Why activated B and T cells differ in their use of nutrients and type of metabolism, despite a similarly high energetic demand is still unclear.

Macrophages are also important mediators of immune responses during infections. They also undergo major metabolic changes to proliferate, produce cytokines and perform phagocytosis. Lipid production is increased in M1-activated macrophages through the mammalian target of

rapamycin (mTOR) signaling pathway, which consequently increases their membrane fluidity and enables the phagocytosis of infected cells. Lipids can also increase phosphatidylcholine production, which activates the NLRP3 inflammasome and production of IL-1β and IL-18 by macrophages [25].

In conclusion, activated immune cells modulate their metabolism to improve their ability to fight pathogens (Figure 2). Part of the systemic metabolic changes observed during infection are therefore thought to enable the optimal nutrient availability to activated immune cells.
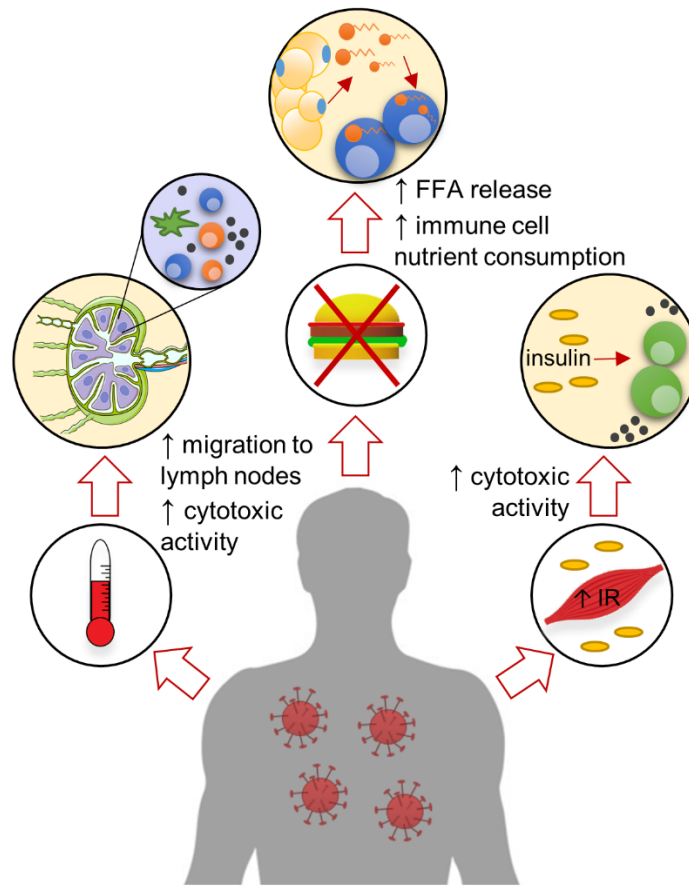
Figure 2. Sickness behavior benefits immune cell activation and defense against pathogens. Fever improves the cytotoxic activity of cells and their migration to lymph nodes. Loss of appetite induces the release of circulating free fatty acids (FFA) from adipose tissue, which are used for energy production in immune cells. Insulin resistance (IR) and reduced glucose uptake induce muscle fatigue, which results in increased systemic insulin levels that promote antiviral T-cell responses.

1.3.   Viruses change the metabolism of host cells to promote their replication.

When a virus enters the cell, it changes key cellular metabolic pathways to promote its replication and spread [26]. These changes are specific for each pathogen, but some common features are typically observed [27]. For example, the metabolic rate of the cell generally increases because of the higher demand for anabolic processes that are required for the formation of viral particles. Viruses such as human cytomegalovirus (hCMV), Epstein-Barr virus, influenza A and dengue virus upregulate cellular glucose transporters to increase glucose uptake and glycolysis [28]. On the other hand, hCMV, herpes simplex virus-1 (HSV-1), and zika virus were shown to increase oxidative phosphorylation to optimize ATP production [28, 29]. In addition to glucose, viruses use glutamine for energy production. For example, vaccinia virus, HSV-1, and adenoviruses increase glutamine uptake and enhance the activities of glutaminase and glutamate dehydrogenase [28-30]. Moreover, α-ketoglutarate, the product of glutaminolysis, can maintain viral growth and energy production when glutamine availability is limited [28, 29, 31]. Other viruses promote lipid synthesis to enable formation of the viral envelope. Lipids can also be used as receptors or co-factors for endosome formation during cell invasion [27]. In hCMV and influenza A infection, it was shown that viral replication is reduced upon the pharmacological inhibition of acetyl-CoA carboxylase (ACC) and fatty acid synthase (FAS) [32]. Therefore, viruses can induce cellular metabolic switches on different levels in order to form suitable machinery for their replication.

Cellular metabolic changes in infected cells can also affect the surrounding environment and, consequently, the metabolism of the whole organ. Following lymphocytic choriomeningitis virus (LCMV) infection of hepatocytes, the urea cycle becomes dysregulated, causing a relative decrease in ornithine in favor of arginine [33]. This shift in systemic nutrient availability has a direct negative impact on the body's ability to fight infection. In vitro treatment of CD8+ T cells with arginine resulted in a poor antiviral response. Notably, arginase treatment in mice caused a reduction in TNF and IFNγ production by CD8+ T cells, which was associated with aggravated liver damage. Thus, the impact of viruses on hepatic urea metabolism appears to be a targeted strategy to impair the local immune response [33].

Viral infection has also been shown to have other systemic impacts on metabolism; for example, LCMV infection increases circulating lipids. Trem2 is a protein that is important for lipid

sensing and animals with specific deficiency of Trem2 in myeloid cells had reduced viral titers and less liver pathology upon LCMV infection [34]. In summary, viral infection changes the metabolism of individual cells. This may lead to metabolic changes in specific organs, and consequently can cause a systemic effect that counteracts sickness behavior.

1.4.   Metabolic diseases modulate the immune response to viral infections.

The detrimental effects of an improper ability to induce sickness behavior upon infection becomes abundantly clear in context of metabolic disease. Metabolic syndrome is associated with symptoms such as elevated blood glucose levels, increased blood pressure, abdominal obesity, dyslipidemia and high cholesterol levels. It is diagnosed when a person has at least three of these symptoms [35]. It is well known that patients with metabolic syndrome more frequently encounter infections, and their symptoms can be more severe, resulting in more complications than in healthy individuals [36]. For example, people with type 2 diabetes (T2D) who already have problems maintaining normal glucose levels often have respiratory, urinary tract, and bacterial infections. In addition, they were shown to have increased rates of infection-caused deaths [37-40]. Recently, it has been observed that people with Severe acute respiratory syndrome coronavirus 2 (SARS-CoV-2) infection have a higher risk of developing serious complications and mortality [41, 42].

Numerous causes are thought to contribute to the worse outcome after viral infection in patients with metabolic disease, including microvascular damage of tissues that disables immune cell infiltration [43], disruptive immune cell skewing due to adipose tissue inflammation [44], and endocrine changes that affect immune cell functionality [45, 46]. Hyperglycemia has been shown to directly cause aberrant immune cell function [47, 48]. Due to chronic hyperglycemia, people with metabolic syndrome fail to induce optimal metabolic changes that occur during sickness behavior, which leads to aberrant antiviral responses. For instance, hyperglycemia during Respiratory Syncytial virus (RSV) infection reduces lung immune cell infiltration, cytokine production and consequently increases viral loads [49]. Similarly, hyperglycemia can directly impair macrophage activation during bacterial *Mycobacterium tuberculosis* infection. As a consequence, the activation of neutrophils and dendritic cells is impaired, resulting in reduced cytokine production. Upon tuberculosis infection in patients with diabetes, it was shown that CD4+ T, CD8+ T, and NK cells have reduced cytotoxicity and cytokine production due to hyperglycemia [50].

7

In summary, metabolic disease negatively impacts the normal immune response to viral infection by preventing the induction of a metabolic state that is optimal for immune cell function, and inhibition of pathogen replication.

1.5. Immune response to viral infection can aggravate metabolic disease.

Metabolic disease negatively impact on the immune system, but conversely activated immune system can also aggravate metabolic diseases. Immune cells accumulate in obese adipose tissue where they respond to stress signals produced by hypertrophic adipocytes. This results in the release of pro-inflammatory cytokines into the blood [44, 51]. Indeed, patients with T2D have a chronic presence of the pro-inflammatory cytokines TNF and IFNγ and it has been shown that these induce systemic insulin resistance [52]. Viral infection, which causes a systemic surge of TNF and IFNγ, was therefore proposed to aggravate metabolic disease. For instance, it is known that infection causes changes in blood parameters, such as glucose levels in patients with diabetes. Therefore, international guidelines recommend screening for infection in patients newly diagnosed with metabolic diseases [53]. Prediabetes is a condition in which patients have elevated glucose levels, but not high enough to be diagnosed with diabetes. If it is not treated on time, patients have a high risk to develop T2D [12, 54]. Infection or sickness behavior exacerbates this condition and can lead to the progression of the disease [12, 55]. For example, infections with hCMV, hepatitis C virus (HCV), and SARS-CoV-2 have been shown to be risk factors for the development of T2D [54].

Insulin receptors are present on the surface of many immune cells, and CD8+ T cells can be stimulated by this hormone to enhance their effector functions [25, 56]. In mice, viral infection induces systemic insulin resistance and increases insulin production which stimulates the anti-viral CD8+ T cell response. Pre-diabetic mice, who have diet-induced insulin resistance, have a higher risk of losing the glycemic control during infection [12].

In diabetes, insulin resistance causes hydrolysis of triglycerides, which induces the release of glycerol and free fatty acids. The liver converts them to glucose and ketones, which can accumulate in the circulation due to insufficient insulin action in these patients. The overproduction of acidic ketones in blood can lead to severe life-threatening ketoacidosis [57]. Infections of the urinary tract, gastrointestinal system, and pulmonary system are the most common

triggers of ketoacidosis in patients with diabetes [58, 59]. The mechanisms underlying infection-induced diabetic ketoacidosis (DKA) are currently unknown; however, understanding them is of great importance for the treatment and prevention of this life-threatening condition. In addition, it is unclear why a metabolic switch towards ketogenesis would benefit the time of infection.

In summary, metabolic adaptations in the context of infection benefit the immune system to fight against the virus, even though the precise mechanism is often not known. However, infection-induced metabolic adaptations can turn into pathology in the context of metabolic disease.

1.6.   Interactions between adipose tissue and the immune system are important for the modulation of systemic metabolism.

For many years, the role of adipose tissue was considered to be only the storage of fat. Currently, it is becoming clear that it is an endocrine organ with multiple functions [51]. It produces anti-inflammatory and immunostimulatory adipokines such as adiponectin and leptin, which are important for glucose, lipid, and energy homeostasis in various tissues [60]. For example, large adipocytes produce less adiponectin and more leptin which is favoring anabolic metabolism [61]. Furthermore, within adipose tissue reside adaptive and innate immune cells which communicate with adipocytes and contribute to the maintenance of physiological conditions by secretion of anti-inflammatory cytokines [51]. Interactions between adipose tissue and the immune system are being investigated, mostly in the context of obesity-induced inflammation and metabolic disorders such as diabetes. In obese conditions, systemic changes in metabolism cause chronic inflammation, which is initiated in adipose tissue. Cells of the immune system, such as macrophages, T and B lymphocytes, NK cells, and NKT cells, infiltrate the fat tissue where they become activated and produce pro-inflammatory cytokines, which further increase inflammation [62, 63].

On the other hand, the role of adipose tissue has not been well investigated in the context of physiological transitory conditions, such as viral infection [64]. The cytokine IL-1β causes downregulation of the GLUT4 glucose transporter in adipose tissue and reduces glucose uptake [65]. A different study has showed that production of the adipokine leptin by adipocytes was increased by stimulation with TNF and IL-1β [66]. As a result, appetite was suppressed, and loss

of body weight occurred. Leptin is also important for the activation and proliferation of NK cells, T cells, and dendritic cells, suggesting that the benefits of its increased concentration in the blood transcend the control of food intake alone [67]. The cytokine TNF was shown to directly increase the expression of adipose tissue hormone-sensitive lipase, an enzyme that hydrolyses triglycerides and induces free fatty acid release [3]. Another pro-inflammatory cytokine, IFNγ was shown to reduce adiponectin production and the response to insulin by human omental adipocytes [68]. IFNγ, TNF and IL-1β are cytokines which are highly induced in the context of viral infection. Whether they also modulate adipose tissue metabolism and systemic lipid levels following infection is currently unknown.

One study showed that infection with human immunodeficiency virus (HIV) causes lipolysis and dysfunction in adipose tissue homeostasis [69]. Similarly, it was observed that infection of monkeys with simian immunodeficiency virus (SIV) reduces the size of their adipocytes [70]. Infection with LCMV induces cachexia in mice which is a result of molecular changes and increased lipolysis in adipocytes. The amounts of triglycerides and free fatty acids in serum are higher in severe infection because of the increased lipid secretion and/or reduced lipid uptake. In addition, infection causes reduction in mRNA expression of *Dgat2* (diacylglycerol O-acyltransferase 2) and *Lpl* (lipoprotein lipase), enzymes involved in triglyceride synthesis and hydrolysis of triglycerides from lipoproteins. These changes are thought to be mediated by IFN-I stimulation of CD8+ T cells [71]. Metabolic changes of adipose tissue are therefore the result of the activation of the immune system, which appears to have a major impact on adipose tissue metabolism. However, cachexia is a pathological condition and only associated with extreme, life-threatening states. It is therefore still unknown why systemic infection modulates adipose tissue metabolism and how this is beneficial for the organism.

In summary, the immune system can directly and indirectly affect adipose tissue metabolism, which modulates systemic nutrient homeostasis during infection. Due to the complexity of immune-fat interactions, we lack knowledge in this field. The purpose of metabolic changes in adipose tissue during viral infection remain unknown, as are key mechanisms how this is established. However, a better understanding of this system appears to be of great importance for the better treatment of patients with severe infection and/or metabolic disease.

2. RESEARCH GOALS

The goal of this research project is to investigate how the activated immune system causes changes in systemic nutrient availability, with a focus on adipose tissue-derived lipids. Moreover, we want to elucidate how these changes benefit the anti-viral response. Better knowledge on these processes is important as it may lead to new opportunities to prevent or treat pathological metabolic conditions such as cachexia, obesity and diabetic complications.

Based on our preliminary data, we hypothesize that immune cells in adipose tissue produce pro-inflammatory cytokines during infection, which modulate adipocyte metabolic gene expression. Its result would be the release of lipids in circulation, to promote immune cell function. Therefore, our main research question is as follows:

Why does viral infection lead to changes in adipose tissue metabolism, and how is this mediated?

To answer the main research question, we subdivided this study into four specific goals:

1. To elucidate what are the physiological changes in adipose tissue/metabolism following mCMV infection.
2. To investigate how the physiological changes in adipose tissue are induced following infection and which cells are responsible for these effects.
3. To investigate what are the physiological roles of changes in adipose tissue metabolism following infection.
4. To investigate how this system derails in the context of diabetic ketoacidosis.

3. MATERIALS AND METHODS

3.1. Materials

3.1.1. Laboratory animals

Animal experiments were conducted in full compliance with Croatian Animal Ethical regulations ("Ordinance on the protection of animals used for scientific purposes", NN 55/2013, which is in accordance with Directive 2010/63/EU of the European Parliament and of The European Council and "Law on animal protection" (NN 135/06, 37/13 and 102/17)) and under a project license of Assoc. Prof. Felix Wensveen. All animal experiments were performed after the approval of our Institute's Animal Ethics Committee (approval no. UP/I-322-01/20-01/41). The experimental mice used in this study were bred and maintained in the specific pathogen-free conditions in the Laboratory of Mouse Engineering and Breeding Facility of the Faculty of Medicine, University of Rijeka (LAMRI). During the experiments, the mice were kept in the Experimental facility in individually ventilated caging system (IVC system) in 12/12-hour light/dark cycles, at 21°C and 50% humidity. All mouse strains used in this study were either generated on a C57BL/6 background or backcrossed at least 10 times with mice on this genetic background. Age matched, 8- to 12-week-old male mice were used, unless stated otherwise. Mouse strains are listed in Table 1.

Table 1. **Experimental mouse strains**

EXPERIMENTAL MOUSE STRAIN	SOURCE	STRAIN CODE
C57BL/6	The Jackson Laboratory	664
B6 CD45.1	The Jackson Laboratory	2014
OT1-1	The Jackson Laboratory	3831
$Ifng^{-/-}$	The Jackson Laboratory	2287
AdiCre/+	The Jackson Laboratory	10803
IFNγR$^{fl/fl}$	The Jackson Laboratory	25394

Ncr1[-GFP/GFP-]	provided by Dr. Ofer Mandelboim (Hebrew university of Jerusalem)	

3.1.2. Viruses

The murine cytomegalovirus (mCMV) virus is BAC (bacterial artificial chromosome) derived. MCMV-pSM3fr-MCK-2fl clone 3.3 in house produced is referred to as mCMV. Virus mCMV-N4 (-SIINFEKL) was generated as described [72]. LCMV Armstrong strain (Armstrong E-350; ATCC) and LCMV-N4 [73] were propagated on baby mouse kidney cells according to standard protocol.

3.1.3. Cell culture mediums

- Dulbecco's modified eagle medium - DMEM

DMEM medium (Pan Biotech, GmbH, Aidenbach, Germany), 3-10% Fetal Calf Serum (FCS) (Pan Biotech), 10 mM HEPES (pH 7.2) (Pan Biotech), 2 mM L-glutamin (Pan Biotech), 105 U/l Penicillin (Pan Biotech), 0.1 g/l Streptomycin (Pan Biotech).

- Roswell park memorial institute medium - RPMI 1640

RPMI medium (Pan Biotech), 3-10% FCS (Pan Biotech), 10 mM HEPES (pH 7.2) (Pan Biotech), 2 mM L-glutamin (Pan Biotech), 105 U/l Penicillin (Pan Biotech), 0.1 g/l Streptomycin (Pan Biotech), β2- mercaptoethanol (Sigma-Aldrich Corporation, St. Louis, Missouri, USA). For experiments with fatty acid free medium, 10% dialyzed FCS was used (Pan Biotech) instead of regular FCS. For in vitro experiments with CD8+ T cells, RPMI medium without glucose was used (Pan Biotech) to dissolve different concentrations of glucose – 1, 2.5, 5, 10, 20, 30 mmol/L (Carl Roth Gmbh+Co KG, Karlsruhe, Germany).

- Cell culture freezing medium

70% RPMI medium (Pan Biotech), 20% FCS (Pan Biotech), 10% dimethyl sulfoxide (DMSO) (Sigma-Aldrich Corporation).

- Flow cytometry medium (FACS medium)

PBS, 1% Bovine serum albumin (BSA) (Thermo Fisher Scientific, Waltham, Massachusetts, USA), 0.1% sodium azide (NaN_3) (Sigma-Aldrich Corporation), 1 mM Ethylenediaminetetraacetic acid (EDTA) (Sigma-Aldrich Corporation).

3.1.4. Buffers

- Magnetic-activated cell sorting (MACS) buffer

PBS, 1% FCS (Pan Biotech), 1 mM EDTA (Sigma-Aldrich Corporation).

- Red blood cell lysis buffer (10x)

140 mM ammonium chloride (NH_4Cl) (Sigma-Aldrich Corporation), 2.7 mM potassium chloride (KCl) (Sigma-Aldrich Corporation), 1.5 mM monopotassium phosphate (KH_2PO_4) (Sigma Aldrich Corporation), 6.5 mM disodium phosphate (Na_2HPO_4) (Sigma-Aldrich Corporation), 0.7 mM calcium chloride ($CaCl_2$) (Sigma-Aldrich Corporation). For working solution (1X) dilute buffer with H_2O.

- Kreb's Ringer phosphate-HEPES buffer (KRP buffer)

Buffer was prepared by mixing Stock 1 (10x) containing: 1.2 M NaCl (Sigma-Aldrich Corporation), 25mM KCl (Sigma-Aldrich Corporation), 12 mM magnesium sulfate ($MgSO_4$) (Sigma-Aldrich Corporation), and sodium dihydrogen phosphate (NaH_2PO_4) (Sigma-Aldrich Corporation) pH=7.4, with Stock 2 (10x) containing: 200 mM HEPES (Pan bitech) and 20 mM $CaCl_2$ (Sigma-Aldrich Corporation) pH=7.4. For working buffer preparation, H_2O was mixed with both buffers to get 1 x solution. This solution was used to prepare 0.1% KRP and 4% KRP buffers with fatty acid free BSA (Carl Roth Gmbh+Co KG).

- 10 x PCR reaction buffer

200 mM Tris/HCl (pH 8.4) (Promega, Madison, Wisconsin, USA), 500 mM KCl (Sigma-Aldrich Corporation).

- Tail lysis buffer

100 mM Tris/HCl (pH 7.5) (Promega), 5 mM EDTA (Sigma-Aldrich Corporation), 0.2% (w/v) SDS (Sigma-Aldrich Corporation), 200 mM NaCl (Sigma-Aldrich Corporation). At the time of use, add 100 μg/ml Proteinase K (Sigma-Aldrich Corporation) to 400 μL of tail lysis buffer.

- TE buffer (Tris-EDTA buffer)

Melt 294.5 g sodium acetate (Sigma-Aldrich Corporation) in 500 ml H_2O, 1 mM EDTA (Sigma-Aldrich Corporation), 10 mM Tris/HCl pH 8.0. Adjust pH with NaOH on 5.5 and add H2O up to 1 L.

- TAE buffer (Tris-acetat-EDTA buffer, 50x)

57.1 ml glacial acetic acid (Sigma-Aldrich Corporation), 242 g Tris base (Sigma-Aldrich Corporation), 100 ml 0.5 M EDTA (pH 8.0) (Sigma-Aldrich Corporation), fill with qH2O up to 100 ml.

3.1.5. Antibodies

Table 2. Antibodies used for flow cytometry

ANTIBODY	SOURCE	IDENTIFIER
Rat Anti-Mouse Monoclonal Antibody TNF alpha FITC (Clone: MP6-XT22)	eBioscience	#11-7321-82
Rat Anti-Mouse Monoclonal Antibody IL-2 PE-Cyanine7 (Clone: JES6-5H4)	eBioscience	#25-7021-82
Syrian hamster Anti-mouse monoclonal KLRG1 FITC (Clone: 2F1)	eBioscience	#11-5893-80

Armenian hamster Anti-mouse Monoclonal Antibody CD3e PE-Cyanine7 (Clone: 145-2C11)	eBioscience	#25-0031-82
Fixable Viability Dye eFluorTM 780	eBioscience	#65-0865-14
Rat Anti- mouse Monoclonal Antibody CD44 APC-eFluor™ 780 (Clone: IM7)	eBioscience	#47-0441-82
Rat Anti-mouse Monoclonal Antibody CD62L PerCP-Cyanine5.5 (Clone: MEL-14)	eBioscience	#45-0621-82
Rat Anti-mouse Monoclonal Antibody IFN gamma PE (Clone: XMG1.2)	eBioscience	#12-7311-82
Rat Anti-mouse Monoclonal Antibody CD4 PE (Clone: GK 1.5)	eBioscience	#12-0041-85
Rat Anti-mouse Monoclonal Antibody CD8a APC-eFluor™ 780 (Clone: 53-6.7)	eBioscience	# 47-0081-82
Armenian hamster Anti-mouse Monoclonal Antibody TCR gamma/delta APC (Clone: GL3)	eBioscience	# 17-5711-82
Mouse Anti-mouse Monoclonal Antibody NK1.1 PerCP-Cyanine5.5 (Clone: PK136)	eBioscience	# 45-5941-82

Rat Anti-mouse Monoclonal Antibody CD11b PE-Cyanine7 (Clone: M1/70)	eBioscience	# 25-0112-82
Armenian hamster Anti-mouse Monoclonal Antibody CD27 PE (Clone: LG.7F9)	eBioscience	# 12-0271-83
Rat Anti-mouse Monoclonal Antibody CD86 Brilliant Violet 605™ (Clone: GL-1)	BioLegend	# 105037
Armenian hamster Anti-mouse Monoclonal Antibody CD80 Brilliant Violet 650™ (Clone: 16-10A1)	BioLegend	# 104731
Rat Anti-mouse Monoclonal Antibody Bcl-6 PE (Clone: BCL-DWN)	eBioscience	# 12-5453-82
7-AAD Viability Staining Solution	eBioscience	# 00-6993-50
Rat Anti-mouse Monoclonal Antibody CD19 PerCP-Cyanine5.5 (Clone: eBio1D3)	eBioscience	# 45-0193-82
Rat Anti-mouse Monoclonal Antibody CD138 APC (Clone: 300506)	eBioscience	# MA5-23553

3.2. Methods

3.2.1. Mouse genotyping

3.2.1.1. DNA isolation from murine tail

Freshly cut or frozen biopsy of approximately 5 mm murine tale was placed in 1.5 mL Eppendorf tube and incubated overnight in a thermo-block at 56 °C with 0,4 mL of Tail lysis buffer and Proteinase K enzyme. Next, the tubes were centrifuged in a small table centrifuge (5 min/12000 rpm) to pellet cellular debris. The supernatant was transferred into a clean tube containing 0.4 mL of isopropanol. DNA was precipitated by mixing with slight rotation of the tube. Samples were then centrifuged (5 min/12000 rpm) and supernatant was removed. The precipitate was washed twice with 0.6 mL of 70% EtOH at to dissolve the residues of precipitated salts. Samples were then centrifuged (5 min/12000 rpm), dried and DNA was dissolved in 150 µL TE buffer and incubated for 15 min at 56°C. Samples were stored at 4°C.

3.2.1.2. Polymerase chain reaction (PCR)

Polymerase Chain Reaction (PCR) was used to amplify a particular part of the DNA molecule. PCR reaction mix contained 10 x reaction buffer, MgCl2 (50 mM) (NEB, Ipswich, Massachusetts, USA), dNTP (5 mM) (Metabion, Munich, Germany), forward primer (Metabion), reverse primer (Metabion), Taq polimerase (0.025 U/µL) (NEB) and qH2O. Volume of each component depended on type of PCR used. Total volume of mix was 50 µL and 1 µL of template DNA was added. PCR reaction was conducted in PCR thermoblock (ProFlex™ PCR system, Applied Biosystems™). This technique was used to check the genotype of in-house bred animals used in the experiments and depending on the genotype, following primers were used (Table 2).

Table 3. List of primers used for PCR

GENE OF INTEREST	PRIMERS
$Ifngr^{fl/fl}$	R: 5`-TTG TTT GAT CCA TTC TTT AAA TTG-3` F: 5`-GCT TCT TTG AAG GGC TGG A-3`

AdiCre/+	SC-1: 5'-GTC CAA TTT ACT GAC CGT ACA-3'
	SC-3: 5'-CTG TCA CTT GGT CGT GGC AGC-3'
OT-1	TCR1 F: 5'-CAG CAG CAG GTG AGA CAA AGT-3'
	TCR1 R: 5'-GGC TTT ATA ATT AGC TTG GTC C-3'
	Ctrl. F: 5'-CAA ATG TTG CTT GTC TGG TG-3'
	Ctrl. R: 5'-GTC AGT CGA GTG CAC AGT TT-3'

3.2.1.3.   Agarose gel electrophoresis of PCR products

Horizontal agarose gel electrophoresis was used to determine the size of the DNA fragments. The 1.5% agarose gel was made by dissolving the agarose (Sigma-Aldrich Corporation) in a boiling TAE buffer. 1 µL of Ethidium-bromide (EtBr) (Sigma-Aldrich Corporation) per 50 ml of cooled gel was added and poured into a gel container. Combs were inserted to enable the formation of the wells after gel polymerization. Molecular-weight size marker was put to the first well to determine the size of the individual DNA fragments. DNA bands were visualized with gelLITE Gel Documentation System (Cleaver Scientific, Rugby, United Kingdom).

3.2.2.   Immune cell isolation

3.2.2.1.   Isolation from spleen

Spleen was harvested and homogenized through a 100 µm cell strainer with 3% DMEM. The homogenate was then centrifuged at 1500 rpm for 5 min. The precipitate was resuspended in 3 mL of red blood cell lysis buffer. Cell suspension was incubated 5 min on ice and 3 mL of 3% DMEM was added. The suspension was centrifuged for 5 min 1500 rpm and the pellet was resuspended in 5 ml of 3 or 10% RPMI.

3.2.2.2. Isolation from VAT

Stromal vascular fraction (SVF) cell isolation from visceral adipose tissue (VAT) was done by cutting the tissue into small pieces and digestion with 0.5 mg/mL Collagenase D (Sigma-Aldrich Corporation) in 5 ml of DMEM medium for 1h, 37°C with shaking at 250 rpm. Tissue pieces were occasionally vortexed to break down adipocytes. After centrifugation and erythrocyte lysis, cells were filtered through a strainer with a pore size 40 μm and resuspended in appropriate volume of medium containing FCS.

3.2.3. Adipocyte isolation from VAT

Adipocyte isolation from VAT was performed by cutting the tissue and digestion in liberase (Roche, Basel, Switzerland) (25 μg/mL) with 4% fatty acid-free BSA in Krebs-Ringer phosphate-HEPES (KRP buffer). Tissue was incubated 45 min at 37°C and shaken at 180 rpm. Suspension was filtered through nylon filter 100 μm and centrifuged at 250 x g 2 min. The washing of adipocytes was done twice in KRP buffer with 0.1% BSA and 2mM EDTA and SVF pellet removed after each washing step. Floating adipocytes were used for further analysis such as RNA isolation with NucleoZOL (MACHEREY-NAGEL, Düren, Germany).

3.2.4. Cell counting

Cell suspensions were counted by using trypan blue stain in 1:1 ratio. Counting was done with Corning Cell Counter (Corning, New York, USA).

3.2.5. Flow cytometry

The results of phenotypic cell assays were obtained by flow cytometry using a FACSVerse (BD), MACSQuant Analyzer 16 (Miltenyi Biotec) and CytoFlex Flow Cytometer (Beckman Coulter, Brea, USA). The data analysis was done with FlowJo software (FlowJo LLC, Ashland, Oregon, USA).

3.2.5.1. Cell surface staining

Flow cytometric analysis was done by fluorophore-labeled antibodies that are specific to certain markers. The single cell suspensions of spleen, VAT or cell lines were prepared and labeling

antibodies were diluted in FACS medium (40 µl), as well as 2.4G2 antibody that blocks FcRII/III (CD16/32) to prevent nonspecific binding of labeled antibodies. After 30 min of incubation at +4°C, the cells were washed with FACS medium, centrifuged 5 min at 4000 rpm and resuspended in 150 µl of FACS medium. Samples were analyzed on the same day.

3.2.5.2. Cytoplasmic intracellular cell staining

For cytoplasmic intracellular staining of cytokines, a kit for fixation and permeabilization of cells was used according to the manufacturers' instructions (Thermo Fisher Scientific). Briefly, cells were stained for surface markers, followed by fixation for 30 min at room temperature with fixation buffer and then washed in permeabilization buffer Perm/Wash. After centrifugation, cells were incubated in 40 µl of antibody mix for 30 minutes at +4 °C. Cells were then washed, centrifuged and resuspended in FACS buffer and measured same or next day.

3.2.5.3. Intranuclear staining

Cells were stained for surface markers, followed by fixation and permeabilization with kit containing diluent and concentrate (Thermo Fisher Scientific) for 30 min at room temperature and then washed in permeabilization buffer Perm/Wash. After centrifugation, cells were incubated in 40 µl of antibody (transcription factor) mix for 1h at +4 °C. Cells were then washed, centrifuged and resuspended in FACS buffer and measured same or next day.

3.2.5.4. Viability dye

Viability dye was used at a dilution factor of 1:1000 in FACS medium together with cell surface staining antibodies. Cells were stained for 30 minutes at +4 °C.

3.2.6. In vitro experiments

3.2.6.1. CD8 T cells

CD8 T cells were purified by positive selection using Ly-2 magnetic beads (Miltenyi Biotec, Cologne, Germany) according to the manufacturer's protocol. Cells were cultured in 10% RPMI described above. For in vitro memory differentiation, 30.000 cells per well in U-bottom 96 well plate were stimulated for 30h with 1ng/mL N4 peptide (Genscript, Piscataway, USA) and 0.5

mg/mL αCD28 (Thermo Fisher Scientific), washed and cultured for an additional 5 days with 50 ng/mL IL-15 (PreproTech). In vitro re-stimulation was done with 10 ng/ml N4 peptide and brefeldin A (Thermo Fisher Scientific).

3.2.6.2. Cell lines

Research was conducted on 2 different cell lines described in Table 4. 3T3-L1 cells were grown on 24 well plate for Bodipy staining or 6 well plate for micro-array analysis or RT-PCR in DMEM with 10% FCS. Adipose differentiation was accomplished by published standard protocol [74]. In biref, three days after plating, when confluence is reached, cells were put in the first differentiation medium containing: 0.5 mM 3-Isobutyl-1-methylxanthine (IBMX) (Sigma-Aldrich Corporation), 1 μg/mL insulin (Novo Nordisk Bagsværd, Denmark), 0.25 μM dexamethasone (Krka, Zagreb, Croatia) and 2 μM rosiglitazone (SmithKline Beecham plc, Brentford, UK) for three days. Next, cells were grown in medium with 1 μg/mL insulin for four days. Finally, cells were 3 days in standard medium. Cells were treated with cytokines (IFNγ and IL-1β 25 ng/ml, TNF 25 pg/ml) (Peprotech) or 4 μM rosiglitazone at the beginning of differentiation and at every medium replacement.

A20 cells (200.000 cells/mL) were grown on 12 well plates in RPMI medium containing 10% FCS dialyzed (PAN-Biotech). Treatment with palmitic, oleic, palmitoleic, vaccenic, linoleic, and stearic acids (Sigma-Aldrich Corporation) was done on each day of the analysis after dissolving them by shaking in the medium containing 10% BSA, fatty acid-free for 20 min at 37°C. On day 3 and were split in the same concentration in a fresh medium with fatty acids and analyzed by flow cytometry.

Table 4. Cell lines

CELL LINE	SOURCE	IDENTIFIER
3T3-L1	ATCC	CL-173
A20	Marc Schmidt-Supprian's lab	/

3.2.6.2.1. Oil red staining

Oil red O dye (Sigma-Aldrich Corporation) staining was done by incubation of 3T3-L1 cells for 10 min in freshly prepared working solution (3 parts Oil red O stock mixed with 2 parts H_2O) in plates in which they grew. Cells were then washed 5 min with distilled water, and nuclei were counterstained with hematoxylin for 3 min. After 5 min washing and 10s incubation in 0.5% HCl, cells were again washed in water 5 min and finally, left in a small amount of water to prevent them from drying. Three pictures were taken per condition and analyzed by ImageJ software.

3.2.6.2.2. BODIPY staining

Cells were trypsinized, washed and stained with viability dye and BODIPY™ 493/503 (Thermo Fisher Scientific) 1.25 µg/mL for 30 min at 4°C.

3.2.6.2.3. Micro array

Total RNA from 3T3-L1 cells was extracted using the NucleoZOL isolation method according to manufacturer instructions. RNA concentration was determined with Nanodrop spectrophotometer (Implen, Westlake Village, USA). Arrays were performed by a commercial partner, according to standard protocol [75]. Data were analyzed using the R2 Genomics analysis and visualization platform (https://r2.amc.nl). The microarray data will be deposited in the Gene Expression Omnibus database upon publication of the manuscript.

3.2.6.2.4. Mito Stress Test

A20 cells were grown in the according to the protocol described under 5.2.6.4. but split on day 2 in culture, and the analysis was done on day 3. Seahorse XF Cell Mito Stress Test Kit (Agilent Technologies, Santa Clara, USA) was used according to the manufacturer's protocol. Assay was performed on Seahorse XFe96 Analyzer (Agilent).

3.2.7. Mouse in vivo experiments

3.2.7.1. Virus infection

Adult animals were infected intravenously (i.v.) with 2×10^5 PFU/mL mCMV or mCMV-N4 in 500 μL of DMEM. Animals were infected intraperitoneally (i.p.) with 1×10^6 IFU of LCMV or LCMV-N4 in 500 μL of DMEM.

3.2.7.2.   Cell depletion, cytokine neutralization and STZ/ALX treatment

For neutralization of NK cells, IFNγ and IL-1β animals were injected the day before infection and on day 2 after the infection i.p. with 500 μg of αNK1.1 (BioX cell; PK136) and αIFNγ (BioX cell; R4-6A2); αIL-1β (10mg/kg) (BioX cell; B122) or appropriate isotype controls. MCC950 (Cayman Chemical, Michigan, USA) was dissolved in PBS in concentration 20 mg/kg and administered 500 μL i.p. in mentioned timepoints, while the control group received PBS. Hyperglycemia was induced with streptozotocin (STZ) (Sigma-Aldrich Corporation) 100 μg/mouse and alloxan (ALX) (Sigma-Aldrich Corporation) 100 ug/mouse dissolved in PBS, 3 and 1 days before, and 2 weeks after mCMV-N4 or LCMV-N4 infection.

3.2.7.3.   Induction of juvenile diabetic ketoacidosis

Three-week-old mice were put on high fat diet (HFD) for 2 weeks. After 16h fasting, mice were injected with STZ/ALX 200 mg/kg each to eliminate pancreatic β-cells and induce diabetes. One group was additionally infected on the same day, and they were subsequently fed with a normal chow diet for 3 days. Blood glucose levels were determined from *v. saphena* with glucometer (SD, Codefree). Ketone levels were also measured with ketone meter (FreeStyle Optium Neo).

3.2.8. Quantitative RT-PCR

Total RNA from 3T3-L1 cells, adipocytes or whole VAT was extracted using NucleoZOL according to the manufacturer protocol. RNA concentration was determined with Nanodrop spectrophotometer. Reverse transcription Core Kit (Eurogentec, Seraig, Belgium) was used to generate cDNA according to the manufacturer instructions in PCR thermoblock (ProFlex™ PCR system, Applied Biosystems™). Real-time PCR was performed with a 7500 Fast Real Time PCR machine (ABI, Waltham, USA) with *Hprt* as housekeeping gene. RT-PCR was done by determining fluorescence of the SYBR Green dye (Eurogentec) according to manufacturer protocol. Primers used in this study are described in Table 3.

Table 5. List of primers used for RT-PCR

GENE OF INTEREST	PRIMERS
Hprt	F: 5'TGAAGAGCTACTGTAATGATCAGTCAAC-3' R: 5'-AGCAAGCTTGCAACCTTAACCA-3'
Pparg	F: 5'- ATTGAGTGCCGAGTCTGTGG-3' R: 3'-ACCTGATGGCATTGTGAGACA-5'
Lpl	F: 5'-TCGTCATCGAGAGGATCCGA-3' R: 3'-TGTTTGTCCAGTGTCAGCCA-5'
Dgat2	F: 5'-GAACGCAGTCACCCTGAAGA-3' R: 3'-TGGGAACCAGATCAGCTCCAT-5'
Ifng	F: 5'-TCTGGAGGAACTGGCAAAAGG-3' R: 3'-TGTGGGTTGTTGACCTCAAACT-5'
Tnf	F: 5'-GAGGCACTCCCCCAAAAGAT-3' R: 3'-ATTTTGAGAAGATGATCTGAGTGTG-5'
Il-1b	F: 5'-GCCACCTTTTGACAGTGATGAG-3' R: 3'-AGCTTCTCCACAGCCACAAT-5'

3.2.9. Histology-H&E staining

Perigonadal VAT or inguinal fat was fixed in 4% formaldehyde (Biognost, Zagreb, Croatia) at least 48h, dehydrated and embedded in paraffin. Sections were deparaffinized with 3 x Xylene 5', 2 x EtOH 100% 3', 1 x EtOH 90% 3', 1 x EtOH 70% 3', 1 x EtOH 50% 3'. Slides were stained with hematoxylin (Thermo Fisher Scientific) 45 min, followed by washing with H_2O and counterstaining with eosin (Thermo Fisher Scientific) 2 min. Dehydration was done as follows: 3' 70% EtOH, 3' 95% EtOH, 3' 100% EtOH, immerse Xylene I, 5' Xylene 2, 5' Xylene 3 and slides were mount with mounting medium. After drying, 3-6 images were taken per tissue. Cell size was quantified as a cell area (Pixels) with ImageJ software plugin Adiposoft.

3.2.10. Immunohistochemistry

For immunohistochemistry, tissue sections were deparaffinized as follows: 3 x Xylene 5', 2 x EtOH 100% 3', 1 x EtOH 90% 3', 1 x EtOH 70% 3', 1 x EtOH 50% 3'. Antigen retrieval was performed by using 1 M sodium citrate buffer (pH=6). Sections were blocked with 3% BSA in PBS and then incubated with primary antibody NCR1-human Fc fusion protein 4 µg/mL (in-house produced) over night at 4°C. Rabbit anti-human biotinylated primary antibody (Jackson ImmunoResearch, IgG) was used for 30 min after endogenous peroxidase block using 0,3% H_2O_2, followed by incubation with streptavidin-POD conjugate (Roche) 45 min. Substrate DAB (Agilent) was added for 45s and reaction stopped with H_2O. Counterstaining was done with hematoxylin for 5 min and dehydration was done as follows: 3' 70% EtOH, 3' 95% EtOH, 3' 100% EtOH, immerse Xylene I, 5' Xylene 2, 5' Xylene 3. When slides were dried, 3-6 pictures were taken per mouse, and analyzed by ImageJ software. We quantified membrane staining by averaging the total signal per pixel from six images per slide and represented it as relative unit (RU).

3.2.11. Mass spectrometry

Blood was collected by heart puncture and plasma was isolated. Lipids were isolated with isopropanol according to the standard protocol [76]. Liquid chromatography-mass spectrometry (LC-MS) was done by commercial partners EMBL Metabolomics Core Facility (Heidelberg, Germany) at high-resolution Q-Exactive Plus (ThermoFisher) mass spectrometer coupled with ultra-high performance liquid chromatography (Vanquish UHPLC) in reverse phase (RP) separation mode.

3.2.12. Densitometry

Density of isolated VAT pads was determined by X-Ray using an In Vivo MS FX Pro imager (Bruker, Billerica, USA) and quantified by MI acquisition and analysis software (Bruker).

3.2.13. Quantification and statistical analysis

Unless otherwise noted, data are presented as mean ± SEM. Statistical significance was determined by either Student's t test or one-way ANOVA with Bonferroni post-testing. Statistical analysis

was performed using GraphPad Prism 8 (GraphPad Software, Inc.). Statistically significant differences were considered with P values of <0.05 (*P < 0.05, **P < 0.01 and ***P < 0.001).

4. RESULTS

4.1. Memory CD8+ T cell function is impaired by both hypo- and hyperglycemia.

As outlined in the introduction, immune cells vary in their requirement of nutrients needed for proliferation, activation and the ability to gain effector functions. To investigate whether low (<5 mmol/L), normal (physiological - 5 mmol/L), or high (>5 mmol/L) glucose concentrations can affect memory CD8+ T cells, we used an in vitro model of OT-1 TCR transgenic CD8+ T cells, previously established in our lab [75]. Purified OT-1 cells were stimulated with N4 (ovalbumin) peptide and αCD28 for 30h. After this, the cells were extensively washed and cultured for 5 more days with IL-15 to differentiate them into memory cells. Memory CD8+ T cells require glucose, as the absence of this nutrient resulted in a low viability. Interestingly, memory CD8+ T cells showed optimal survival under low to physiological concentrations of glucose, whereas hyperglycemia (>5mM) had a negative impact. Moreover, cells cultured under high glucose concentrations preferentially obtained a central memory-like phenotype (CD44- CD62L+). Low glucose concentrations pushed cells towards an effector memory phenotype (CD44+ CD62L-) (Figure 3a).

To determine whether glycaemia impacts memory T cell functionality, cells were restimulated in vitro with N4 peptide and cytokine production was measured by flow cytometry. Functionality of cells cultured with high glucose concentration was greatly impaired, because IFNγ, TNF and IL-2 production was strongly reduced (Figure 3b). To determine whether we could recapitulate this phenotype in vivo, we injected mice with the toxic glucose analogues streptozotocin/alloxan (STZ/ALX). These compounds specifically delete pancreatic beta cells, thus abrogating insulin production and causing hyperglycemia. In wild type (WT) (CD45.2$^+$) control or STZ/ALX-treated mice, we transferred 10^4 OT-1 cells (CD45.1$^+$) and after 1 day infected them with a murine cytomegalovirus strain expressing the N4 epitope of ovalbumin (mCMV-N4). After 42 days when memory was formed, OT-1 cells from these mice were re-stimulated in vitro with the N4 peptide. Cytokine production was reduced in memory CD8+ T cells isolated from hyperglycemic mice (Figure 3c). Next, OT-1 cells were transferred to mice with or without STZ/ALX injection and infected with mCMV-N4. 43 days later, they were re-infected with lymphocytic choriomeningitis virus expressing N4 (LCMV-N4). After 7 days, cytokine production was measured by in vitro re-stimulation of splenic OT-1 cells with N4 peptide. These

results showed reduced IFNγ production of secondary effector cells under hyperglycemic conditions, while TNF and IL-2 production did not change between the groups (Figure 3d). Finally, control or STZ/ALX mice were transferred with OT-1 cells and 1 day later infected with LCMV-N4. After one month, NK cells were depleted and mice were infected with mCMV-N4. Mice with memory CD8+ T cells formed in a hyperglycemic environment had significantly increased viral titers, comparing to the control animals (Figure 3e). In summary, even though memory CD8+ T cells need normal glucose levels for proper function, high concentrations of this nutrient are detrimental in fighting against viral infection. Therefore, increased availability of other nutrients than glucose could be more important for the functionality of immune cells in infection.
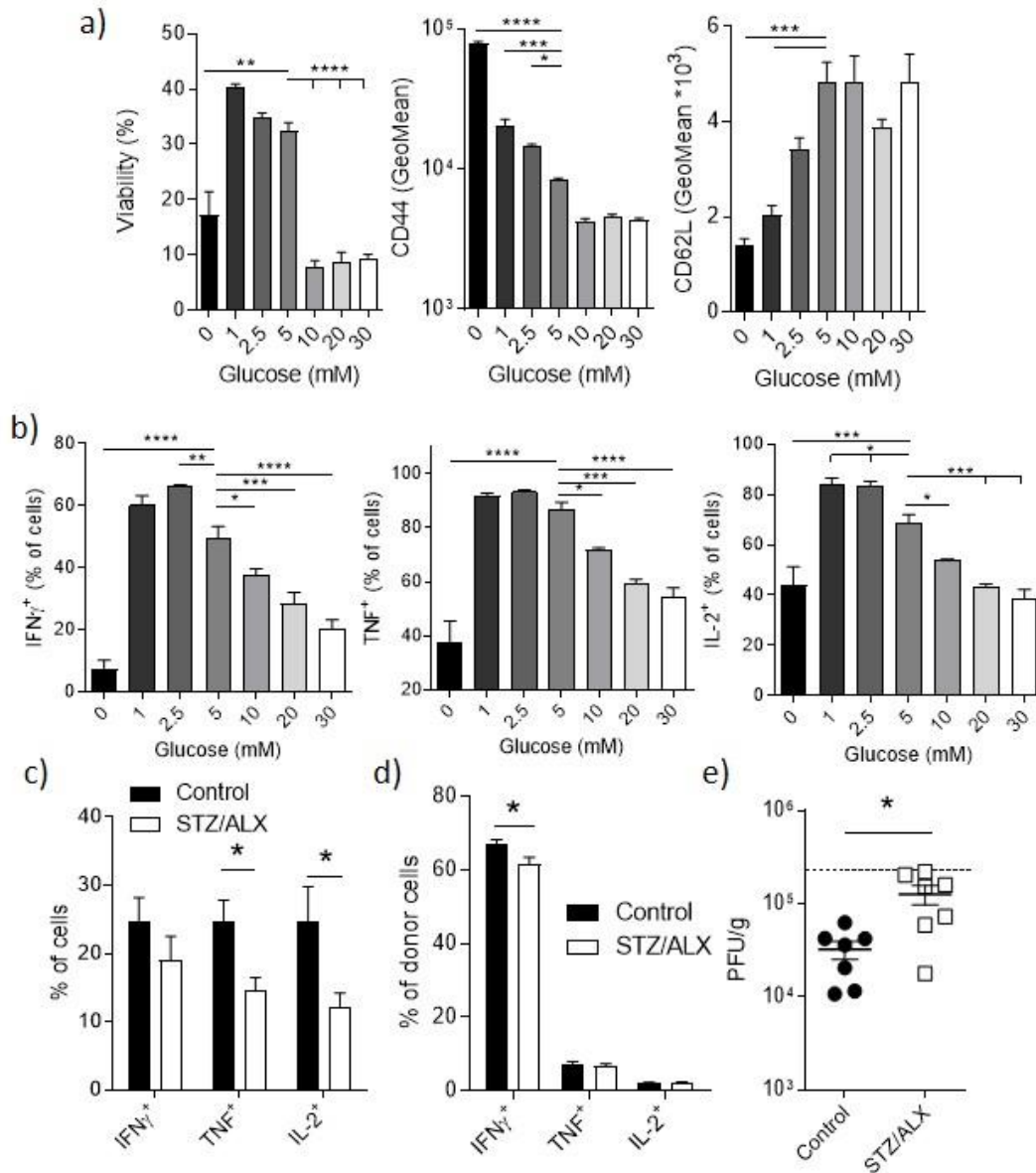
Figure 3. Hyperglycemia has a negative impact on memory CD8+ T cell functionality during viral infections. a-b) Purified CD8+ OT-1 cells were stimulated in vitro with N4 peptide and αCD28 for 30 h in media containing different glucose concentrations (low, medium, and high). The cells were then washed and incubated with IL-15 for 5 days to form memory cells. Flow cytometry analysis of a) viability and expression of surface markers CD44 and CD62L; b) cytokine production after re-stimulation with N4 peptide. c-d) 10^4 OT-1 (CD45.1^{+}) cells were transferred to WT recipients (CD45.2[+]). Hyperglycemia was induced in these animals by injection of streptozotocin (STZ) 100 µg/mouse and alloxan (ALX) 100 ug/mouse 3 and 1 days before and 2 weeks after mCMV-N4 infection. 1 day before infection c) 42 days after priming, CD45.1[+] donor OT-1 cells were detected and re-stimulated with N4 peptide to measure cytokine production. d) Control or STZ/ALX-treated mice were infected with mCMV-N4 and 43 days later, recall was

done with LCMV-N4. OT-1 cells were re-stimulated and cytokine production was measured. e) Control or STZ/ALX-treated mice were transferred with 10^4 OT-1 cells, next day infected with LCMV-N4. One month later, NK cells were depleted and animals were infected with mCMV-N4 the day after. Liver viral titers were determined after 4 days by standard plaque assay. Viral titer of mice who did not receive OT-1 cells are represented as dashed line. Data shows means ± standard error of the mean (s.e.m.). For all panels, shown is one of at least two experiments with similar results. Indicated are statistical significances at ANOVA a-b), Student t test e-g) and Mann-Whitney test h) * $p < 0.05$, ** $p < 0.01$.

4.2. Infection with mCMV leads to a transient reduction in adipocyte size.

Besides glucose, immune cells require other nutrients, such as lipids, to execute their function and fight viral infection. We therefore wanted to investigate the impact of viral infection on adipose tissue biology. Male C57BL/6 mice were infected with mCMV i.v. and adipocyte cell size of VAT was determined on hematoxylin-stained sections. We observed a significant decrease in average adipocyte size, which was most prominent 3 days after infection. This effect was transient, as adipocytes regained their original size after 7 days (Figure 4a). To investigate whether this is an mCMV-specific effect, we infected mice with another virus, LCMV strain Armstrong. Again, we observed a decrease in adipose tissue size, which indicates that adipocyte shrinking is a general response to viral infection (Figure 4b).

It is important to note that the used dose of virus causes an infection which resembles a normal acute infection in humans associated with a physiological sickness behavior response. To investigate whether mCMV infection-induced changes in adipose tissue size are the result of changes in appetite, which is a main sickness behavior, we weighed the mice and measured their daily food consumption. Infected animals did not show a significant reduction in either their body weight gain or food consumption within 3 days after infection (Figure 4c and data not shown). Furthermore, to investigate whether forced administration of nutrients can prevent the effect of mCMV infection on adipocyte size, mice were provided with water supplemented with 5% glucose for 3 days. Body weight gain and food consumption were not affected, but they had smaller adipocytes than the non-infected animals (Figure 4c-d and data not shown). Thus, adipose tissue size reduction following infection occurs despite the ample availability of systemic nutrients.

To confirm the histological analysis, the density of the adipose tissue was measured by x-ray. The density of adipose tissue was reduced in comparison with that of the control animals (Figure 4e). Interestingly, the overall weight of VAT did not change (Figure 4f). In summary, 3 days after mCMV infection, mice did not change body weight, appetite, or VAT weight, whereas adipocyte size and adipose tissue density were reduced. This occurred despite the ample availability of nutrients. These findings indicate that infection specifically changes adipocyte metabolism.
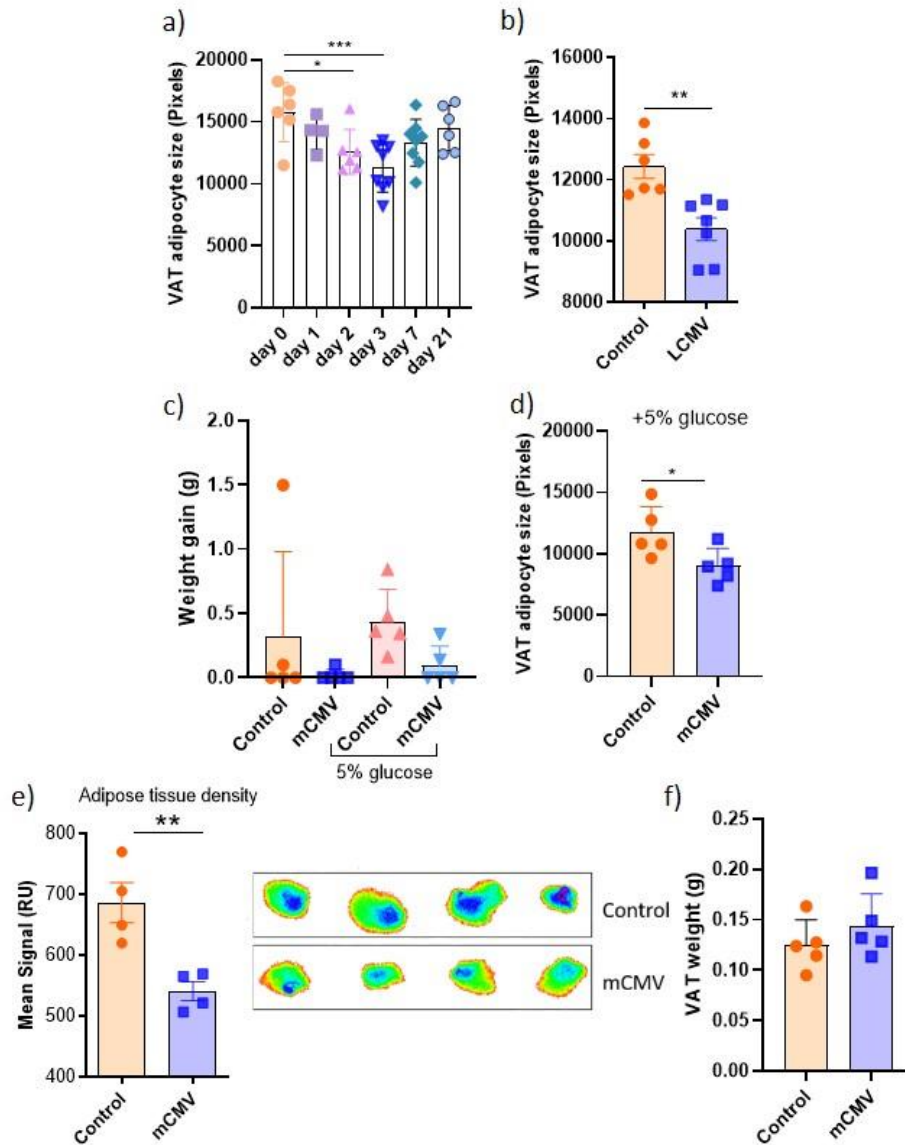
Figure 4. Viral infection induces reduction in size of visceral adipocytes. a) Animals were infected and at the indicated time points, VAT cell size was quantified using hematoxylin-stained tissue slides. b) Three days after LCMV infection, VAT adipocyte size was analyzed. c) Body weight gain of control, mCMV and control and mCMV mice treated with 5% glucose in water for 3 days. d) Adipocyte size of control and mCMV mice treated with 5% glucose in water for 3 days. e) The density of adipose tissue at the indicated time point was measured by x-ray and quantified as the mean signal on day 3 after mCMV infection. f) The weight of the VAT was determined as the average weight of two fat pads on day 3 after mCMV infection. Data shows means ± standard error of the mean (s.e.m.). For all panels, shown is one of at least two experiments with similar results. Indicated are statistical significances at ANOVA a) and Student t test * $p < 0.05$, ** $p < 0.01$.

4.3. The pro-inflammatory cytokine IFNγ is responsible for metabolic changes in adipocytes in vitro.

After showing that mCMV infection induces metabolic changes in adipose tissue, we investigated whether these changes are a consequence of specific proinflammatory cytokines produced during infection. First, we measured expression levels of cytokines important for antiviral response including IFNγ, TNF and IL-1β in total VAT lysates by RT-PCR. As expected, their expression was highly induced after mCMV infection, especially IFNγ (Figure 5a). Primary adipocytes are very difficult to manipulate in vitro. Therefore, to test the impact of cytokines on adipocyte biology, we used a previously described in vitro model of 3T3-L1 fibroblasts that can differentiate into adipocytes when grown under specific cell culture conditions [74]. Briefly, cells were grown in 10% DMEM for 3 days, after which the medium was replaced with differentiation medium containing 3-isobutyl-1-methylxanthine, rosiglitazone, dexamethasone, and insulin. Three days later, they were placed in a second differentiation medium containing insulin for 4 days, followed by 2 days in normal 10% DMEM. Firstly, cells were treated with the cytokines IL-1β and IFNγ. Oil red O staining of lipids and quantification of red areas with ImageJ software showed that IFNγ and IL-1β significantly reduced the amount of lipids in adipocytes (Figure 5b-c). To confirm these results, BODIPY fluorescent dye was used to stain lipids and cells were analyzed bv flow cytometry. Using this assay, the cytokine IL-1β and additionally TNF did not show an impact on lipid composition, but IFNγ significantly reduced BODIPY signal in adipocytes (Figure 5d-f).
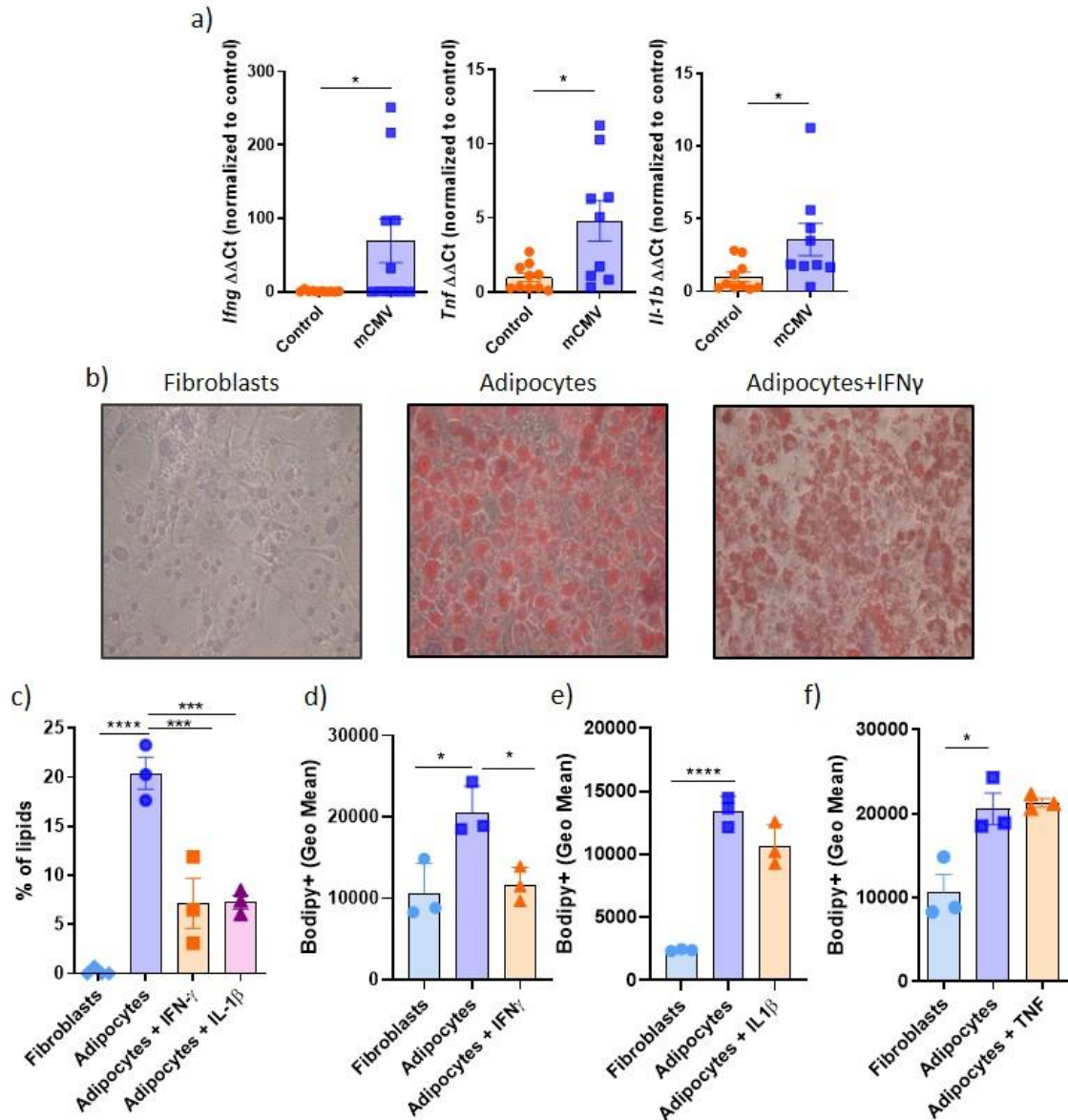
Figure 5. IFNγ reduces lipid content in 3T3-L1 adipocytes in vitro. a) RT-qPCR analysis of cytokine mRNA levels in total VAT lysates 3 days after mCMV infection. The data were normalized to those of the control group. b-f) 3T3-L1 fibroblasts were differentiated into adipocytes and treated with IFNγ, IL-1β (both 25 ng/ml), or TNF (25 pg/ml). b) Oil red O staining of lipids and c) quantification of red areas using ImageJ software. d-f) BODIPY staining of lipids was analyzed by flow cytometry. Fluorescence is shown as the geometric mean signal. Data shows means ± standard error of the mean (s.e.m.). For all panels, shown is one of at least two experiments with similar results. Indicated are statistical significances at ANOVA c-e) and Student t test a) * $p < 0.05$, ** $p < 0.01$.

4.4. The pro-inflammatory cytokine IFNγ is responsible for metabolic changes in adipose tissue and systemic fatty acid release in mice.

We questioned whether IFNγ or IL-1β are important for changes in VAT adipocyte size following mCMV infection in vivo. Therefore, mice were injected with neutralizing antibodies for IFNγ, IL-1β, or with the NLRP3 inflammasome inhibitor MCC950 prior to infection. Adipocytes were analyzed three days later by histology. These cytokines were selected because IFNγ showed a significant impact on lipid accumulation in vitro according to oil red staining (Figure 5 d-e). IL-1β, however, did not have an impact on adipocyte size compared to untreated mCMV mice, nor did MCC950 treatment (Figure 6a). Strikingly, IFNγ neutralization in infected mice reversed adipocyte size to the levels observed in the control group (Figure 6b). Together, these results indicate that IFNγ, but not IL-1β, is important for the shrinking of adipocytes during mCMV infection in vivo.

After showing that IFNγ reduces adipocyte size, our next question was if lipids are released into the circulation upon viral infection. To test this hypothesis, we analyzed the plasma lipid profile of animals three days after mCMV infection. Infected animals treated with IFNγ-neutralizing antibodies were included to determine the specific effect of this cytokine. The total lipidomic profile showed an increase of many lipid species during infection compared to non-infected mice (Figure 6c). In particular, free fatty acids levels in serum were significantly increased upon mCMV infection (Figure 6d). Notably, we observed an increase in oleic acid (Figure 6d), which is not only normally found in mouse adipose tissue [77], but also present in blood plasma in humans [78]. Strikingly, when IFNγ was neutralized, the changes in lipid profile were almost completely abrogated (Figure 6e). Altogether, the data shows that IFNγ produced during mCMV infection induces free fatty acid release from adipocytes.
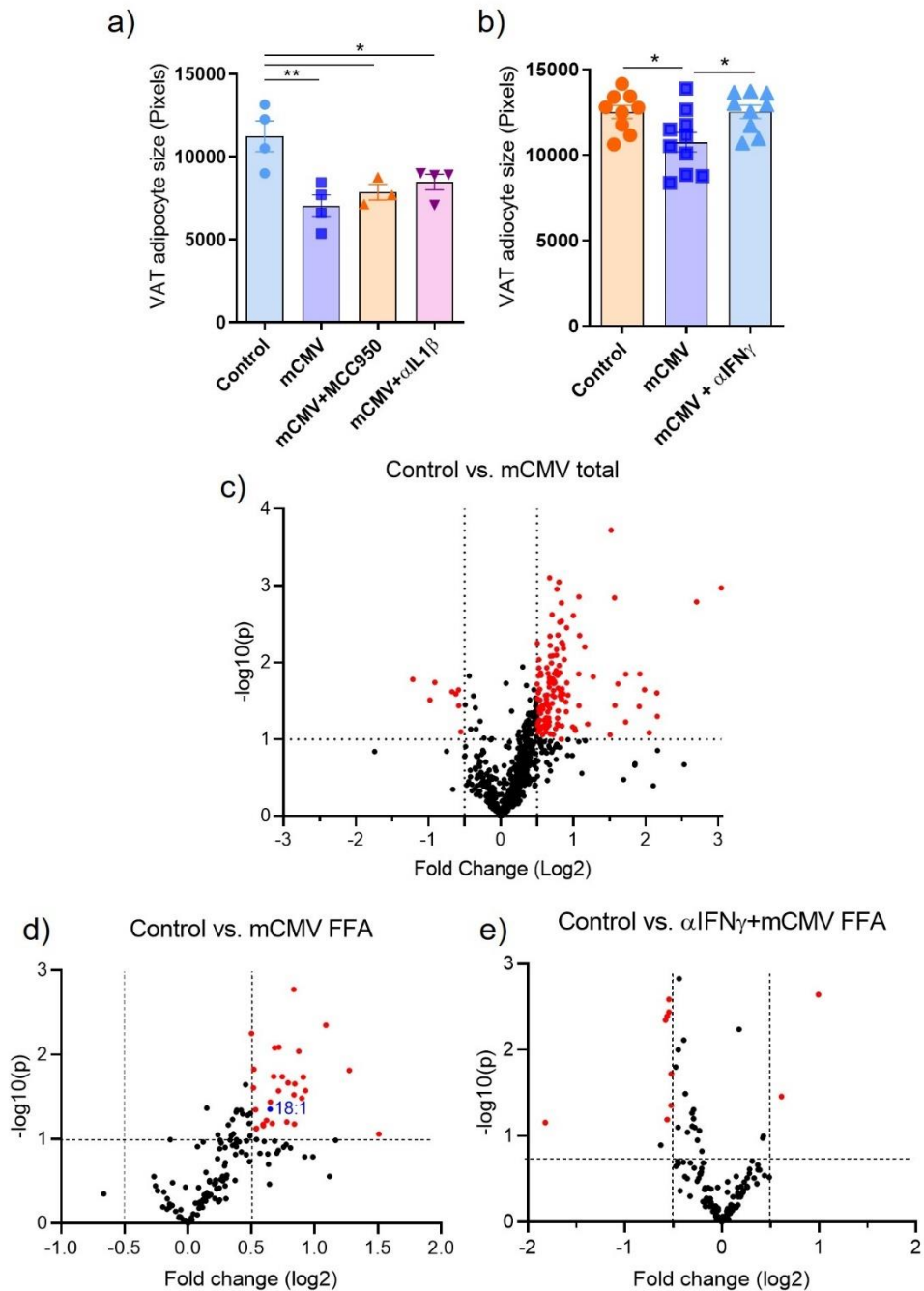
Figure 6. IFNγ and not IL-1β, is responsible for release of lipids by adipose tissue in circulation. a-b) C57BL/6 mice were injected with αIL-1β, αIFNγ, or the inflammasome inhibitor MCC950, followed by mCMV infection. Animals were analyzed after 3 days. a) Histological analysis of adipocyte size in mice in which IL-1β was neutralized or its production inhibited and b) IFN-γ neutralization. c-e) Blood plasma was isolated, and isopropanol-based isolation of lipids

was performed for LC-MS detection of fatty acids 3 days after mCMV infection of untreated mice or animals that had received neutralizing αIFNγ antibodies. Red dots indicate significantly changed lipid species. c) total lipids in control vs. mCMV animals; d) free fatty acids (FFA) in mCMV mice in comparison to the control; e) significantly abundant or reduced free fatty acids in mCMV mice without IFNγ in comparison to control mice. c) Blue dot: 18:1 represents oleic acid.

Data shows means ± standard error of the mean (s.e.m.). For all panels except mass spectrometry data, shown is one of at least two experiments with similar results. Indicated are statistical significances using (a,b) ANOVA or (c-e) student t test on log-transformed data * $p < 0.05$, ** $p < 0.01$.

4.5. IFNγ changes adipocyte metabolism by reducing activity of the PPARγ transcription factor.

To determine the underlying mechanisms by which IFNγ induces free fatty acid release from adipose tissue, we first tested whether this cytokine has a direct effect on adipocytes in vivo. We used AdiCre/+ IFNγR$^{fl/fl}$ to specifically delete this receptor on adipocytes. Indeed, when adipocytes lacked the ability to sense IFNγ their size was not affected by mCMV infection (Figure 7a). To elucidate how IFNγ mediates changes in adipose tissue metabolism, we investigated the changes in gene expression profile of 3T3-L1 adipocytes after IFNγ stimulation by micro-array. Differential pathway expression analysis showed that the peroxisome proliferator-activated receptor-gamma (PPARγ) signaling pathway was significantly downregulated in cells treated with IFNγ (Figure 7b). PPARγ is an important regulator of systemic glucose and lipid metabolism, adipocyte differentiation and - biology. It regulates the expression of many genes, such as *Lpl*, which hydrolyzes triglycerides in lipoproteins, and *Dgat2*, which is important for triglyceride synthesis [79, 80]. Microarray analysis showed that these genes were downregulated in IFNγ-treated adipocytes compared to those in control adipocytes (Figure 7c). RT-PCR analysis confirmed the significant downregulation of transcription of the *Lpl* and *Dgat2* genes (Figure 7d and data not shown). In addition, when cells were cultured in the presence of rosiglitazone, an agonist for PPARγ, IFNγ-mediated inhibition of *Lpl* expression was partially reverted (Figure 7e).

Finally, to confirm that IFNγ mediates its impact on adipose tissue through modulation of the PPARγ signaling cascade following infection in vivo, we performed RT-PCR analysis of mRNA isolated from adipocytes. RT-PCR analysis showed reduced *Lpl* expression in infected animals, confirming the previous in vitro results. Notably, animals deficient for IFNγ did not show a reduction in *Lpl* expression of adipose tissue following mCMV infection (Figure 7f). Overall, our results indicate that IFNγ alters adipocyte metabolism by inhibiting activity of the PPARγ transcription factor. This results in reduced expression downstream target genes involved in lipogenesis and therefore a net loss of nutrient content.
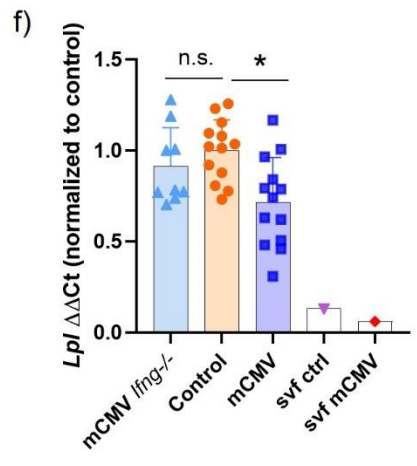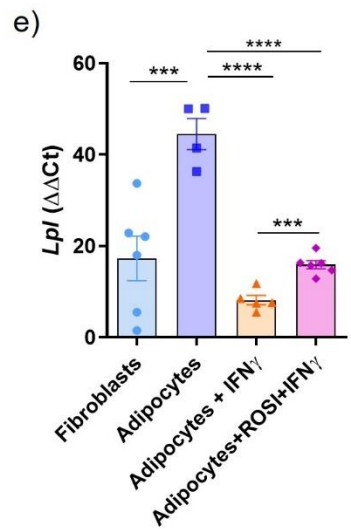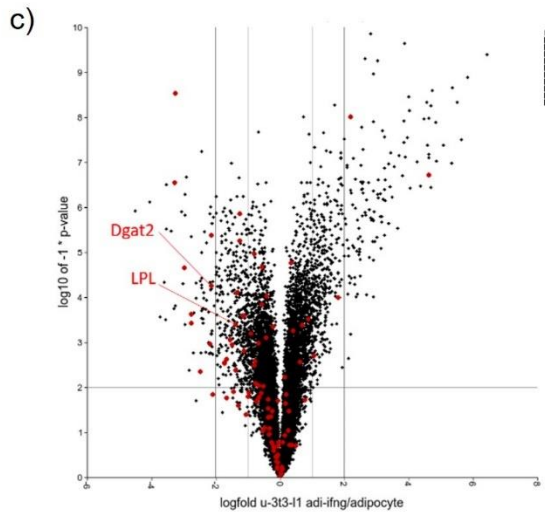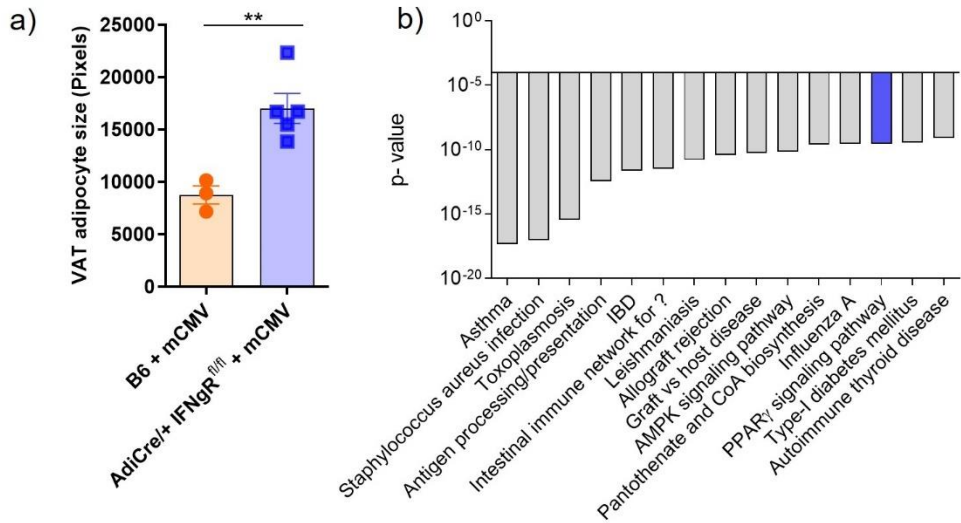
Figure 7. IFNγ produced in infection changes adipocyte metabolism through PPARγ transcription factor. a) VAT cell size was analyzed in infected mice that lack the IFNγ receptor on adipocytes (AdiCre/+ IFNγR$^{fl/fl}$) and wild-type controls. b) RNA was isolated from undifferentiated, differentiated and differentiated IFNγ-treated 3T3-L1 cells and analyzed by microarray. Shown is differential KEGG-pathway expression analysis. c) Vulcano plot of differentially expressed genes. Red dots represent genes directly regulated by PPARγ. d) RT-PCR of *Pparg* expression in 3T3-L1 cells. e) *Lpl* mRNA expression in 3T3-L1 adipocytes treated with IFNγ, PPARγ agonist rosiglitazone or a combination of the two. f) RT-PCR analysis of *Lpl* expression in adipocytes isolated from VAT in control or infected animals. g) *Lpl* mRNA levels in adipocytes isolated from the VAT of indicated groups with (mCMV) or without (control) mCMV infection. Svf (stromal vascular fraction) represents non-adipocyte mRNA levels, used as a control for the purity of the isolated adipocytes. For all panels, shown is one of at least two experiments with similar results. Indicated are statistical significances at ANOVA d-f) and Student t test a) * $p < 0.05$, ** $p < 0.01$.

4.6. NK cells are responsible for IFNγ production and changes in adipose tissue during mCMV infection.

After showing that IFNγ induces adipocyte changes upon viral infection, our following question was which immune cells produce this cytokine in VAT. IFNγ is predominantly produced by lymphocytes and we therefore first measured the kinetics of different lymphocyte subtypes in this tissue during mCMV infection. Three days after mCMV infection NK cells were most abundant in VAT, while numbers of CD8+ T, CD4+ T, γδ T and NKT cells increased in numbers only at later time points (Figure 8a). We therefore hypothesized that NK cells may be most important for mediation of adipocyte cell reduction following viral infection.

To investigate the activation status of these cells in VAT following infection, we analyzed their phenotype by flow cytometry over time. On day 0 and 1 NK cells were not activated yet. As expected, three and six days after the infection they were mostly CD11b+, CD27+ and KLRG1+ indicating an activated phenotype. At ten days, NK cells had gained a phenotype that had almost reverted to the one they had before infection. (Figure 8b). Notably, day three after infection coincided with the maximum viral titer (Figure 8c), minimal adipocyte size and maximal NK cell activation status and cell numbers in VAT.

NK cells are known to play an important role in the pathological inflammatory processes in obese adipose tissue [44]. We therefore hypothesized that they mediate metabolic changes in this tissue following infection through their secretion of IFNγ. To answer this question, we measured IFNγ production by different cells in the infected VAT and found that NK cells are the dominant source of this cytokine on day 3 after infection (Figure 8d). To confirm this, we measured mRNA levels of *Ifng* in the VAT of infected animals with depleted NK cells. We observed reduced levels of *Ifng* transcripts in the VAT of NK cell depleted animals when compared to the infected isotype control-treated mice (Figure 8e). Finally, histological adipocyte size quantification was performed in mCMV mice in which NK cells were depleted with antibodies or in animals treated with isotype control antibodies. NK cell loss prevented a reduction in adipocyte size upon infection, indicating that NK cells are mediating nutrient release from adipocytes (Figure 8f).
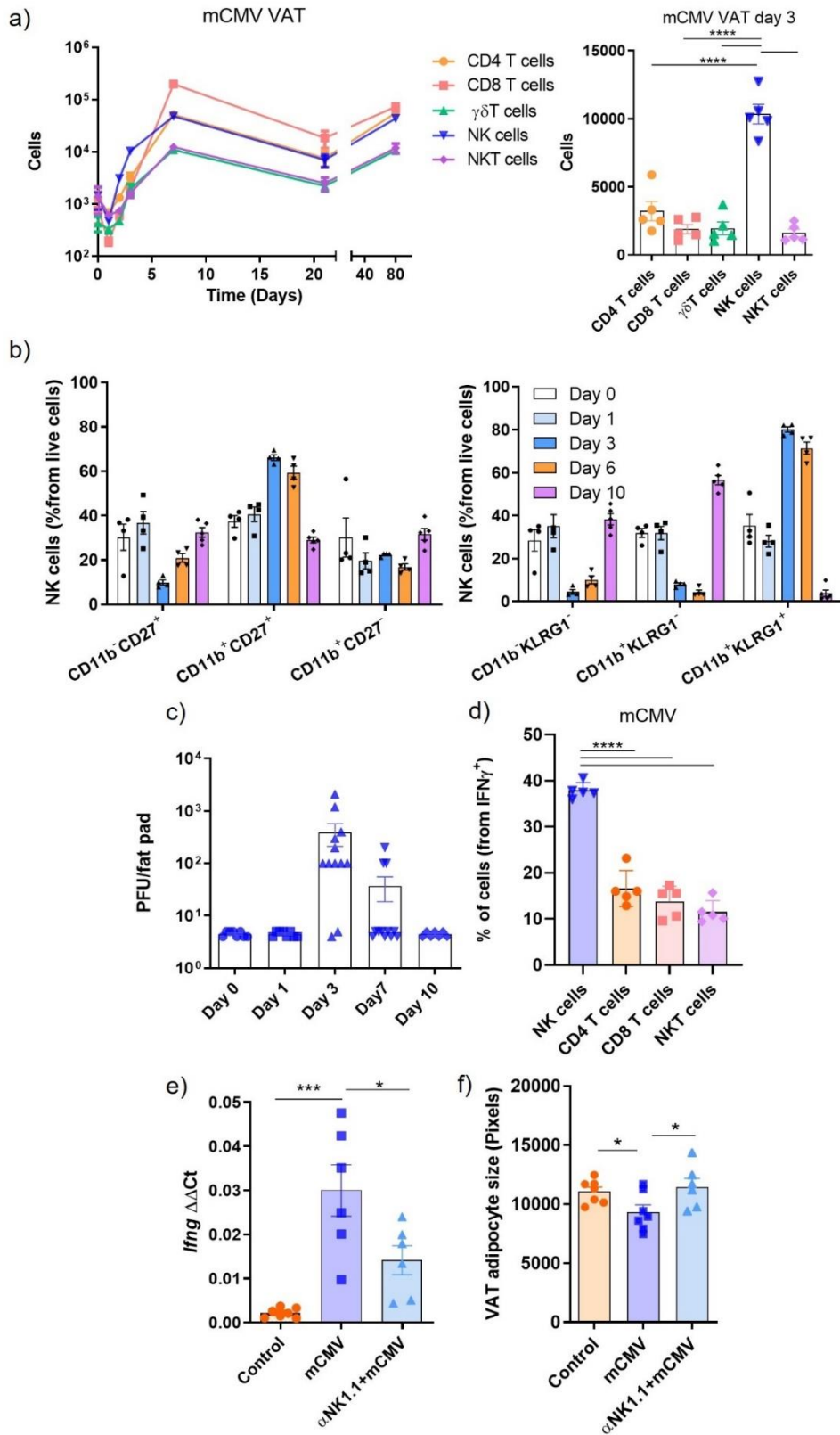
Figure 8. NK cells are responsible for IFNγ production and changes in adipose tissue during mCMV infection. a) Kinetics of immune cell subsets in the VAT after mCMV infection. Right panel shows cell numbers on day 3. b) Phenotype of VAT NK cells over time after mCMV infection. c) Viral titers in VAT at different timepoints determined with plaque assay. d) Percentage of NK, CD4 T, CD8 T and NKT cells within the IFNγ-producing cell fraction in the VAT on day 3 after mCMV infection. e) *Ifng* mRNA levels of in control, mCMV and mCMV mice treated with αNK1.1 depleting antibody. f) Adipocyte size in uninfected, infected, and infected animals with depleted NK cells. For all panels, shown is one of at least two experiments with similar results. Indicated are statistical significances at ANOVA * $p < 0.05$, ** $p < 0.01$.

4.7. The NCR1 receptor is important for metabolic changes in VAT.

Previously, we have shown that obesity-induced inflammation results in the upregulation of NCR1 ligands in VAT [44]. Hence, our goal was to investigate the presence of these ligands in VAT during mCMV infection. Tissue sections were analyzed by immunohistochemistry using the NCR1 fusion protein, which allows visualization of ligands for this receptor. Infection with mCMV resulted in significant upregulation of ligands for NCR1 (Figure 9a). Therefore, to confirm that indeed NCR1 is important for NK cell activation and subsequent changes in adipocytes, we measured the adipocyte size in $Ncr1^{-GFP/GFP-}$ mice, which lack the NCR1 receptor, after mCMV infection. We observed that $Ncr1^{-GFP/GFP-}$ mice failed to mediate adipocyte shrinkage in response to mCMV infection (Figure 9b). Thus, NK cells mediate metabolic changes in adipocytes following infection through recognition of adipose tissue stress by the NCR1 receptor.
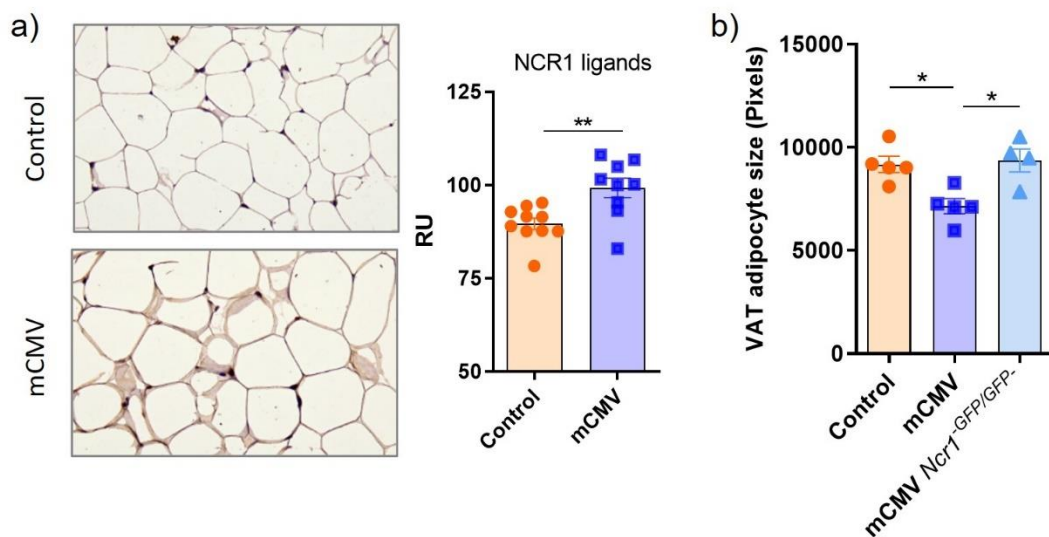
Figure 9. NCR1 mediated NK cell activation is important for VAT metabolic changes 3 days after mCMV infection. a) VAT tissue sections of control and mCMV-infected mice were stained with NCR1 fusion protein, which detects ligands for this receptor, and counterstained with hematoxylin. Quantification of DAB signal was done in ImageJ software. We quantified membrane staining by averaging the total signal per pixel from six images per slide and represented it as relative unit (RU). b) VAT adipocyte size of control mice as well as WT and $Ncr1^{-GFP/GFP-}$ mice infected with mCMV. For all panels, shown is one of at least two experiments with similar results. Indicated are statistical significances at ANOVA b) and Student t test a) * $p < 0.05$, ** $p < 0.01$.

4.8. Oleic acid promotes activation of A20 B cell lymphoma cells in vitro.

As shown above, mass spectrometry data detected different fatty acids released by adipocytes following IFNγ engagement. Because germinal center B cells preferentially use fatty acid oxidation as a primary source of energy [24], we hypothesized that increased free fatty acid release by adipocytes following infection promotes the B cell response. To investigate this, we used the A20 mouse B cell lymphoma cell line as a model. First, we tested the impact of several of the most abundant fatty acids normally found in adipose tissue, including palmitic, oleic, palmitoleic, vaccenic, linoleic, and stearic acids on the activation of these cells. Cells were cultured in RPMI medium containing 10% dialyzed FCS, indicating that they do not contain any fatty acids in the serum. Fatty acids were bound to fatty-acid-free BSA and dissolved in the same medium. After 3 days in culture, oleic acid was the only fatty acid that upregulated the expression of the co-stimulatory ligands CD80 and CD86. This was associated with a concomitant reduction in expression of the Bcl-6 transcription factor, which is a negative regulator of these molecules [81] (Figure 10a-c). Oleic acid was indeed taken up by these cells, as indicated by increased BODIPY staining following its incubation with A20 cells (Figure 10d).

We hypothesized that OA promotes the activation status of A20 cells by stimulation cellular metabolism. To investigate if oleic acid can change the metabolic rate of these cells, the Seahorse Mito Stress Test was performed after 3 days of fatty acid treatment (Figure 10e). The Mito Stress Test is a method used for the measurement of mitochondrial functionality by determining the oxygen consumption rate (OCR). First, oligomycin was injected to inhibit ATP synthase after the basal respiration measurement. This change in OCR measurement is represented by ATP production. Next, Carbonyl cyanide-4 (trifluoromethoxy) phenylhydrazone (FCCP) was injected to disrupt the proton gradient and mitochondrial membrane potential. In this step, cells are able to reach the maximum respiration rate. Finally, rotenone and antimycin A was injected in the well to shut down mitochondrial respiration. We calculated ATP production and basal respiration, and both were increased following oleic acid treatment, which was concentration-dependent (Figure 10f). FCCP did not increase respiration over that under basal conditions, indicating that these cells do not have spare respiratory capacity, which is to be expected of a cell line.

In conclusion, fatty acids, such as oleic acid, may be important for the early activation of B cells and promotion of their role as antigen-presenting cells. Oleic acid possibly activates B cells by mediating changes in their metabolic rate.
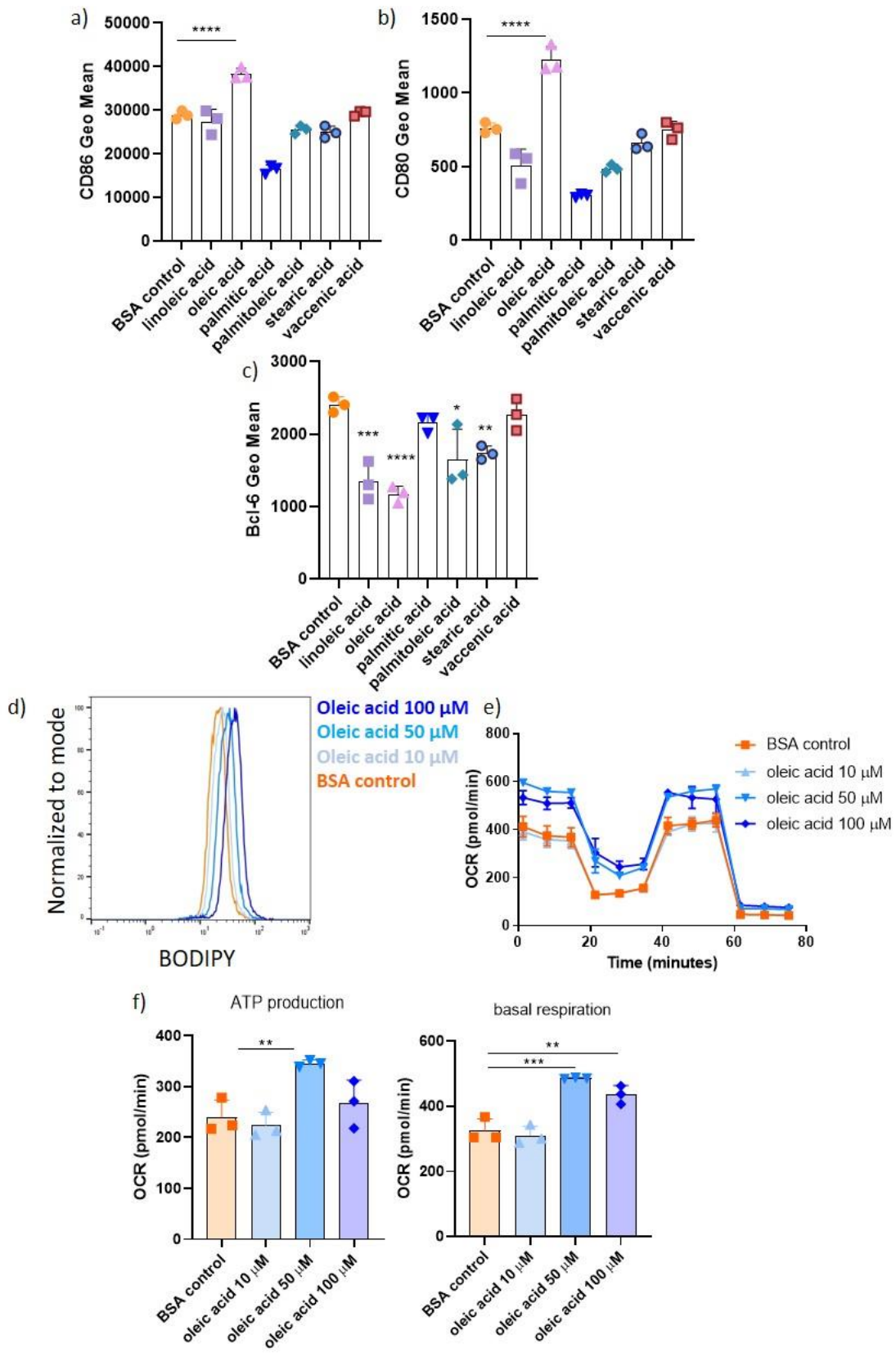
Figure 10. Oleic acid induces CD80 and CD86 expression and increases basal respiration rate in A20 B cell line. a-c) A20 cells were seeded at a concentration of 200.000 cells/mL and cultured in 10% RPMI without fatty acids. Cells were cultured for 3 days and treated with different fatty acids at a concentration of 100 µM. CD80, CD86 and Bcl-6 geometric mean was measured by flow cytometry. d) BODIPY lipid staining in cells treated with increasing concentrations of oleic acid. d) Mito Stress Test was done by using Seahorse XF analyzer and the oxygen consumption rate (OCR) was determined in cells treated with oleic acid 10, 50, 100 µM or control. e) Quantification of ATP production and basal respiration calculated of data shown in d. For all panels, shown is one of at least two experiments with similar results. Indicated are statistical significances at ANOVA * $p < 0.05$, ** $p < 0.01$.

4.9. IFNγ deficiency impairs early B cell activation following viral infection.

Finally, we questioned whether IFNγ is important for the early activation of B cells. WT mice or animals deficient for IFNγ were infected with mCMV and their activation was analyzed after three days. We observed that infection caused an increase in the expression of CD86 in early activated CD138+CD19+ cells, which did not occur in animals lacking IFNγ (Figure 11). Thus, IFNγ promotes the early activation of B cells following viral infection in vivo.

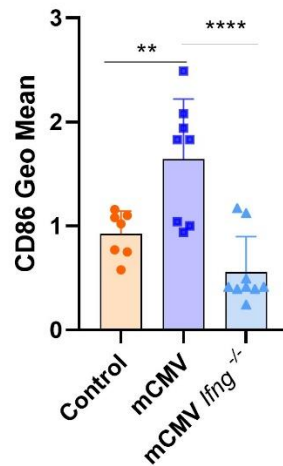**Figure 11. IFNγ deficiency impairs early B cell activation following viral infection.** WT and *Ifng*^{-/-} mice were infected with mCMV. After three days, CD86 expression was quantified on early activated (CD138+CD19+) B cells. Shown is one of at least two experiments with similar results. Indicated are statistical significances using ANOVA test. ** $p < 0.01$, *** $p < 0.001$.

4.10.   Diabetic ketoacidosis is not aggravated by the mCMV infection.

Diabetic ketoacidosis (DKA) is an acute life-threatening condition in people with diabetes and its occurrence often coincides with infection. To investigate if mCMV infection can aggravate diabetic ketoacidosis, we used a known model of juvenile DKA in mice [82]. Three-week-old mice were put on HFD for 2 weeks. After 16h fasting, mice were injected with STZ/ALX 200 mg/kg each to eliminate pancreatic β-cells and induce diabetes. One group was additionally infected on the same day, and they were subsequently fed with a normal chow diet for 3 days. Even though these mice develop hyperglycemia (Figure 12a) and ketosis, mCMV infected STZ/ALX mice have same ketone levels as uninfected animals (Figure 12b).

Whereas in the STZ/ALX group one mouse died, in the infected group two animals did not survive until the final time point. Therefore, in this mouse model of diabetic ketoacidosis mCMV infection does not impact the blood ketone levels in diabetic animals, but more evidence is necessary to confirm if it negatively impacts the mortality rate, in comparison to uninfected mice.
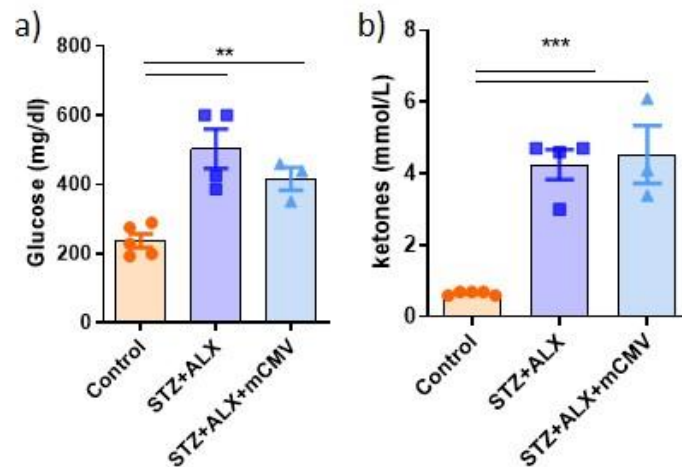
Figure 12. Diabetic ketoacidosis is not aggravated during the mCMV infection. a-b) Three week old C57BL/6 mice were fed with high fat diet (HFD) for 2 weeks. After the 16h fasting, one group was injected with STZ/ALX 200mg/kg of each and other infected with mCMV. Animals were fed with normal chow diet for following 3 days, when a) blood glucose; and b) ketone levels were measured with glucometer and ketone meter. One animal in STZ/ALX and 2 in mCMV STZ/ALX did not survive until time point of interest. Shown is one of at least two experiments with similar results. Indicated are statistical significances using ANOVA test. ** $p < 0.01$, *** $p < 0.001$.

5. DISCUSSION

The immune system interacts with adipose tissue under pathological conditions such as obesity and T2D. Also, it is known that severe infection may lead to cachexia, which is the pathological depletion of nutrients from adipose tissue, irrespective of nutrient intake [71]. However, little is known about the physiological interactions between immune cells and adipocytes upon activation of the immune system. In particular, it is unclear how the immune system affects adipose tissue biology in transient, acute viral infections. Here we show that infection with mCMV activates NK cells in VAT through the NCR1 receptor though upregulation of its ligands on adipocytes. NK cells then produce high amounts of the cytokine IFNγ, which targets adipocytes directly and drives them to downregulate PPARγ, a master regulator of adipose tissue biology [83]. This results in the reduction in adipocyte cell size and the efflux of fatty acids and other lipids into the circulation. These lipids stimulate the metabolism of B cells and promote their activation. Fatty acids released upon viral infection therefore appear to be an important energy source for the early activation of B lymphocytes and their ability to activate T cells. Thus, we elucidate a new mechanism how the immune system controls lipid homeostasis upon its activation, with the purpose to better fight viral infection.

Glucose was shown to be a key nutrient for many activated immune cells, yet paradoxically its levels do not change significantly upon infection [12]. Importantly, we observed that systemic high glucose availability does not benefit the immune system, and even inhibited memory CD8+ T cell functionality. It is well known that different immune cells vary in their requirements for nutrients to fulfill the energetic needs, and that this changes based on their function and activation status [15]. Patients with T2D have chronic hyperglycemia and therefore high availability of glucose to immune cells. CD8+ T cells preferentially use glucose as a source of energy upon activation [84]. At the same time, these cells are known to function optimally even at very low glucose concentrations [85]. Therefore, it was not clear how hyperglycemia impacts memory CD8+ T cell functionality during viral infections. We found that a low or physiological concentration range of glucose was beneficial for memory CD8+ T cell response, while high concentrations showed detrimental effects both in vitro and in vivo. How this effect is mediated is currently unknown but may be the result of changes in AMP-activated protein kinase (AMPK) and mTOR activation. These molecules are differentially regulated by changes in energy availability

and are essential for normal memory CD8+ T cell function [86, 87]. Dysregulation of these molecules following hyperglycemia may therefore lead to suboptimal immune responses. Oure findings are an example how homeostasis of nutrients is essential also for optimal function of the immune system. It is therefore likely that any anti-diabetic therapy which lowers the blood glucose levels, could be beneficial for memory CD8+ T cell response in people with T2D.

Nutrients other than glucose, such as lipids can also be an important source of energy for immune cells. So far, a lot of attention has been given to changes in immune cell metabolism following their activation. For example, is known that memory CD8+ T cells rely more on fatty acid oxidation, while effector CD8+ T cells depend on glycolysis to fulfill their energetic needs [88]. However, how these changes in metabolic requirements of immune cells are accommodated by changes in systemic metabolism is less well known. Even though infection-induced sickness behavior typically manifests with reduced food intake [71], paradoxically our immune cells have a higher demand for nutrients. Upon mCMV inoculation we observed that VAT adipocytes transiently reduce their size and release lipids into circulation. This was not associated with pathological changes in general physiology, as body weight, food consumption or VAT weight remained unchanged. This suggests that the observed changes are a well-regulated physiological response to infection. Indeed, the viral dose we have used does not induce severe sickness behavior in mice, such as the one observed in high doses of LCMV, which causes irreversible cachexia [71]. Therefore, instead of increasing the food intake to enable nutrient access, the body appears to use endogenous nutrients such as lipids to fuel the activation of immune cells. This system reduces availability of nutrients such as glucose, which is a preferential energy source of virally infected cells [89]. At the same time, it causes a shift in systemic nutrient availability that is beneficial for some activated immune cells. Indeed, it is known that lipids can improve activation of immune cells. For example, palmitate induces chemokine expression through the NF-κB signaling pathway in macrophages [90]. Fatty acid synthesis and uptake were shown to be important for acquiring of effector functions by T cells, mostly in the context of the tumor microenvironment [91]. Germinal center B cell and plasma B cell formation was reduced in B cell specific PPARγ knockout mice [92], and fatty acids are known to be important ligands for this receptor [93]. Thus, our results identify a new type of sickness behavior in which NK cells regulates systemic lipid availability in order to benefit the immune response.

In the steady state, anti-inflammatory immune cells are located in adipose tissue where they maintain homeostatic immune-suppressive conditions [94]. During metabolic stress, the frequency of immune cells in adipose tissue increases and the formation of a pro-inflammatory environment is initiated [51]. We show that also upon systemic mCMV infection immune cells accumulate in the VAT. We found that NK cells peaked in numbers three days after infection, while CD8+ T cells are most abundant after seven days, when the adipose tissue cell size was mostly restored to its original size. Immune cell infiltration is not unexpected considering that adipose tissue is a nutrient rich environment, suitable for immune cells and for pathogens as well. Additionally, it is a widely distributed organ, which is highly metabolically active and can rapidly adjust its nutrient in- and efflux. As such, it can serve as a reservoir for viruses such as HIV, human adenovirus Ad-36, influenza A and cytomegalovirus [95]. HIV, for example, infects macrophages and CD4+ T cells which accumulate in adipose tissue, but not in adipocytes [70, 95]. The underlying reasons why viruses would persist in this tissue even though it is not infecting adipocytes directly are not clear, but a rapid access to energy stored in the form of lipids seems plausible. Metabolic changes we observe in VAT early after mCMV infection, are induced through VAT induction of NCR1 ligands, in order to activate this receptor on NK cells. Moreover, we previously showed that NCR1 ligands are overexpressed in obese adipose tissue and are responsible for the proliferation and IFNγ production in NK cells [44]. The inflammation in VAT can therefore have two purposes: recruitment of immune cells to protect the tissue and induction of changes in lipid metabolism to benefit the immune system.

Pro-inflammatory cytokines such as IFNγ and IL-1β are highly produced in obese VAT [51]. Metabolic stress can be responsible for NLRP3 inflammasome activation and IL-1β production, which leads to local and systemic inflammatory response [96]. Macrophages were shown to be important for the induction of inflammation and recruitment of other immune cells, through the production of IL-1β [51]. As a consequence, the number of IFNγ producing cells also increases rapidly, in particular NK cells [44, 51]. Conversely, IFNγ produced by NK cells in adipose tissue polarizes tissue resident macrophages, thus potentiation their ability to produce IL-1β [44]. Both cytokines can therefore contribute to insulin resistance and development of metabolic disease. Our data has shown that IFNγ and IL-1β are produced in VAT after mCMV infection. Even though IL-1β had a minor impact on adipocyte biology in vitro, it did not have a significant impact on the adipocyte cell size in mice. On the other hand, IFNγ had a direct impact on adipocyte

cell size and on metabolic gene expression. Hence, IFNγ appears to communicate directly to the adipocytes, whereas IL-1β likely signals to the local immune system.

The mechanisms by which the cytokine IFNγ can change adipocyte biology are not completely resolved. One of the major signaling pathways regulating adipocyte biology and function is the janus kinase/signal transducer and activator of transcription (JAK/STAT), which can be activated by IFNγ [97]. In addition, *Pparg* is a STAT1 target gene and it was shown in 3T3-L1 adipocytes that STAT1 binds to the IFNγ response elements in the *Pparg2* promoter [98, 99]. Similarly, it also binds to IFNγ response elements in *Lpl* gene promoter region [97]. In human adipocytes in vitro, IFNγ impairs lipid storage, reduces expression of *Pparg* and its target genes *Adipoq*, *Glut4* and *Lpl* [100]. We have showed that this cytokine downregulates the PPARγ signaling pathway in 3T3-L1 adipocytes and downregulates genes under the control of the PPARγ transcription factor, such as *Lpl* both in vitro and in vivo, upon infection. Therefore, IFNγ produced in infection downregulates PPARγ, likely through the JAK/STAT signaling pathway.

Different immune cells could benefit from lipids released upon viral infection. A recent study has shown that germinal center B cells use oxidative phosphorylation for energy. This is in contrast to, for example, activated CD8+ T cells and macrophages, which preferentially use glycolysis to fulfill their energetic needs [24, 89]. Moreover, another study demonstrated that upon activation, B cells show an increase in genes regulating oxidative phosphorylation and the tricarboxylic acid cycle but surprisingly, not genes related to glycolysis. Glucose deficiency did not impact B cell functionality, but disruption of oxidative phosphorylation reduced its activation and differentiation to plasma cells [101]. Our results indicate that oleic acid could be one of the fatty acids specifically released from adipose tissue upon infection to optimally increase the ATP production and activation of B cells. Oleic acid is the major fatty acid present in human circulation which can be used as energy or for the formation of cell membranes [102]. The immuno-modulatory capacity of this fatty acid has also been observed because it can increase the proliferation of human lymphocytes in vitro [103]. Moreover, oleic acid originating from adipocytes can increase the proliferation of CD4+ T cells upon antigen encounter [104]. However, oleic acid has not been investigated in the context of early B cell activation. Our findings indicate that it specifically promotes oxidative phosphorylation in these cells as we have showed that it increases the oxygen consumption rate of A20 B cells in vitro.

B cell activation is characterized by downregulation of Bcl-6 and upregulation of the co-stimulatory molecules CD80 and CD86 [81, 105]. CD80 and CD86 are expressed on the surface of antigen presenting cells and can induce activation of CD8+ T cells, through the binding to CD28/CTLA4, which are the most potent co-stimulatory receptors on these cells [106]. Additionally, B and T cells were shown to closely interact around 3 days after antigen encounter in the plane of the T-cell B-cell zone in the lymph nodes [107]. Palmitic acid was previously shown to decrease the antigen presentation during antigen presenting-cell T-cell interaction, while oleic acid has prevented the detrimental effect of palmitate [108], indicating that it could be important in B-cell T-cell interactions. Our findings indicate that fatty acid metabolism is rate limiting for the full activation of B cells and that increased availability of oleic acid helps with this process.

Physiological metabolic changes during viral infection can aggravate symptoms or induce complications in patients with diabetes [12, 55]. Diabetic ketoacidosis has been recognized as one of the metabolic complications induced by infection [58]. Surprisingly, our results show that mCMV infection does not impair ketosis in diabetic mice, in comparison to uninfected animals. One of the possible explanations is that mice have a faster or more adaptable metabolism than humans [109], and therefore are less prone for the accumulation of ketone bodies in the circulation. Nevertheless, our findings mildly suggest that infection may increase the mortality rate in mice suffering from diabetic ketoacidosis. This would be in line with human studies, which showed that patients with diabetic ketoacidosis had an increased mortality rate when infected with SARS-CoV-2 [110]. However, it remains to be investigated whether these observations are linked to changes in lipid efflux from adipocytes following infection.

In summary, sickness behavior which is normally beneficial can become detrimental when it is induced in a metabolically stressed environment.

6. CONCLUSION

Adipose tissue is one of the main organs controlling systemic lipid availability. Immune cells reside in adipose tissue, where they have an important role in maintaining adipose tissue homeostasis [51]. However, it was mostly unknown how the immune system interacts with adipose tissue during acute viral infection and how it may be involved in the development of infection-induced sickness behavior. Our findings reveal a mechanism by which NK cells are activated in response to viral infection, modulate adipocyte biology and cause metabolic changes in this organ. One purpose of these physiological changes is to promote early B lymphocyte activation and help them to fight against the virus through increased release of oleic acid. Therefore, our main findings are (Figure 13):

- Cytokine production by memory CD8+ T cells is impaired under conditions of hyperglycemia, suggesting that other nutrients such as lipids may be more acutely needed during infection for optimal immune cell function.
- In response to infection, adipose tissue induces expression of ligands for the activating NK cell receptor NCR1.
- Following NCR1 stimulation, NK cells in adipose tissue produce high amounts of the cytokine IFNγ.
- IFNγ directly targets adipocytes and induces their downregulation of the key adipogenic transcription factor PPARγ and its target genes.
- As a consequence of metabolic changes in adipocyte, fatty acids are released from adipose tissue into the blood following infection.
- Nutrient release by adipocytes is observed both after mCMV or LCMV infection, indicating that it is a general response to viral infection.
- Oleic acid (OA) is one of the primary fatty acids being released by adipocytes in response to infection. OA was particularly potent in activating the A20 B cell line, resulting in an increase of basal respiration and ATP production.
- Potentiation of the activation status of A20 cells resulted in upregulation of CD80/CD86 and reduction in the expression of Bcl-6 transcription factor, thus increasing their costimulatory potential.
- Deficiency of IFNγ impairs B cell activation in vivo.

- Infection with mCMV does not aggravate ketosis in diabetic mice, but it may increase the mortality rate.

In summary, our data identifies a new mechanism via which the immune system and adipose tissue interact in context of viral infection.
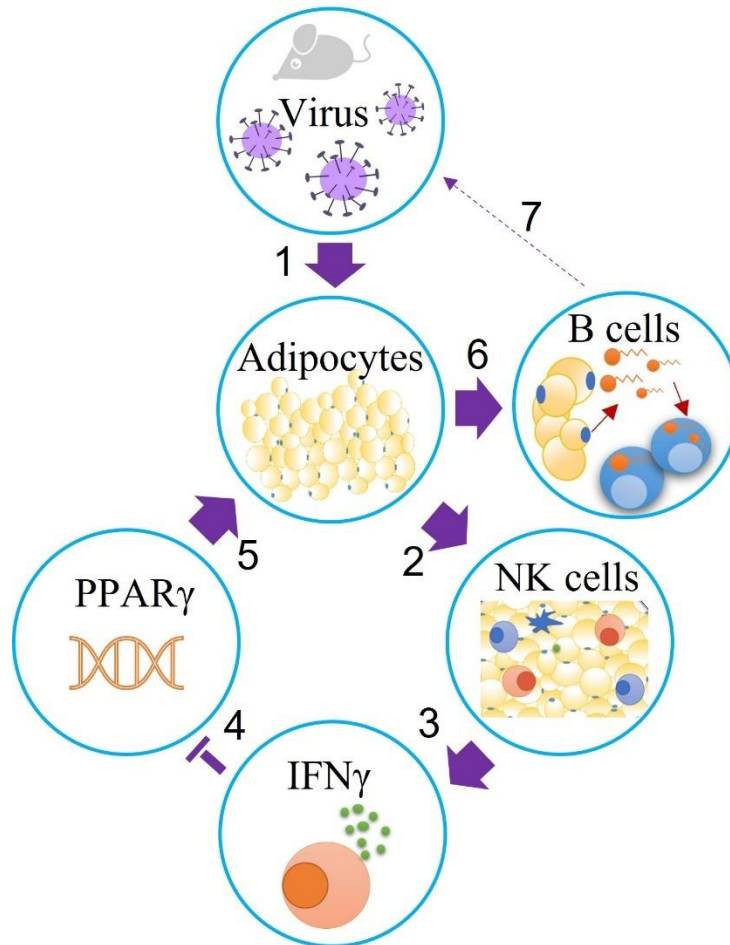
Figure 13. Graphical abstract of our key findings. The systemic viral infection impacts visceral adipose tissue (1), because different immune cells infiltrate in the tissue and we find that NK cells are highly abundant (2). They produce cytokine IFNγ which is downregulating the main transcription factor important for adipocyte biology, PPARγ (4). This results with the adipocyte cell reduction (5), and the efflux of free fatty acids which could be important for early B cell activation (6) and their anti-viral response (7).

7. LITERATURE

1.   Wensveen FM, Jelencic V, Polic B. NKG2D: A Master Regulator of Immune Cell Responsiveness. Frontiers in immunology. 2018;9:441.
2.   Vollmer-Conna U, Fazou C, Cameron B, Li H, Brennan C, Luck L, et al. Production of pro-inflammatory cytokines correlates with the symptoms of acute sickness behaviour in humans. Psychological medicine. 2004;34(7):1289-97.
3.   Tizard I. Sickness behavior, its mechanisms and significance. Animal health research reviews. 2008;9(1):87-99.
4.   Machado NLS, Bandaru SS, Abbott SBG, Saper CB. EP3R-Expressing Glutamatergic Preoptic Neurons Mediate Inflammatory Fever. The Journal of neuroscience : the official journal of the Society for Neuroscience. 2020;40(12):2573-88.
5.   Evans SS, Repasky EA, Fisher DT. Fever and the thermal regulation of immunity: the immune system feels the heat. Nature reviews Immunology. 2015;15(6):335-49.
6.   Prajitha N, Athira SS, Mohanan PV. Pyrogens, a polypeptide produces fever by metabolic changes in hypothalamus: Mechanisms and detections. Immunology letters. 2018;204:38-46.
7.   Schmidt KD, Chan CW. Thermoregulation and fever in normal persons and in those with spinal cord injuries. Mayo Clinic proceedings. 1992;67(5):469-75.
8.   Lin C, Zhang Y, Zhang K, Zheng Y, Lu L, Chang H, et al. Fever Promotes T Lymphocyte Trafficking via a Thermal Sensory Pathway Involving Heat Shock Protein 90 and alpha4 Integrins. Immunity. 2019;50(1):137-51 e6.
9.   Townsend L, Dyer AH, Jones K, Dunne J, Mooney A, Gaffney F, et al. Persistent fatigue following SARS-CoV-2 infection is common and independent of severity of initial infection. PloS one. 2020;15(11):e0240784.
10.   Norheim KB, Jonsson G, Omdal R. Biological mechanisms of chronic fatigue. Rheumatology. 2011;50(6):1009-18.
11.   Capuron L, Gumnick JF, Musselman DL, Lawson DH, Reemsnyder A, Nemeroff CB, et al. Neurobehavioral effects of interferon-alpha in cancer patients: phenomenology and paroxetine responsiveness of symptom dimensions. Neuropsychopharmacology : official publication of the American College of Neuropsychopharmacology. 2002;26(5):643-52.
12.   Sestan M, Marinovic S, Kavazovic I, Cekinovic D, Wueest S, Turk Wensveen T, et al. Virus-Induced Interferon-gamma Causes Insulin Resistance in Skeletal Muscle and Derails Glycemic Control in Obesity. Immunity. 2018;49(1):164-77 e6.
13.   Aviello G, Cristiano C, Luckman SM, D'Agostino G. Brain control of appetite during sickness. British journal of pharmacology. 2021;178(10):2096-110.
14.   Francesconi W, Sanchez-Alavez M, Berton F, Alboni S, Benatti C, Mori S, et al. The Proinflammatory Cytokine Interleukin 18 Regulates Feeding by Acting on the Bed Nucleus of the Stria Terminalis. The Journal of neuroscience : the official journal of the Society for Neuroscience. 2016;36(18):5170-80.
15.   Alwarawrah Y, Kiernan K, MacIver NJ. Changes in Nutritional Status Impact Immune Cell Metabolism and Function. Frontiers in immunology. 2018;9:1055.
16.   Kedia-Mehta N, Finlay DK. Competition for nutrients and its role in controlling immune responses. Nature communications. 2019;10(1):2123.
17.   Kelly B, O'Neill LA. Metabolic reprogramming in macrophages and dendritic cells in innate immunity. Cell research. 2015;25(7):771-84.
18.   Muehlenbein MP, Hirschtick JL, Bonner JZ, Swartz AM. Toward quantifying the usage costs of human immunity: Altered metabolic rates and hormone levels during acute immune activation in men. American journal of human biology : the official journal of the Human Biology Council. 2010;22(4):546-56.

19.   Carr EL, Kelman A, Wu GS, Gopaul R, Senkevitch E, Aghvanyan A, et al. Glutamine uptake and metabolism are coordinately regulated by ERK/MAPK during T lymphocyte activation. Journal of immunology. 2010;185(2):1037-44.
20.   Cham CM, Driessens G, O'Keefe JP, Gajewski TF. Glucose deprivation inhibits multiple key gene expression events and effector functions in CD8+ T cells. European journal of immunology. 2008;38(9):2438-50.
21.   Straub RH, Cutolo M, Buttgereit F, Pongratz G. Energy regulation and neuroendocrine-immune control in chronic inflammatory diseases. Journal of internal medicine. 2010;267(6):543-60.
22.   Balmer ML, Ma EH, Bantug GR, Grahlert J, Pfister S, Glatter T, et al. Memory CD8(+) T Cells Require Increased Concentrations of Acetate Induced by Stress for Optimal Function. Immunity. 2016;44(6):1312-24.
23.   Allen CD, Okada T, Cyster JG. Germinal-center organization and cellular dynamics. Immunity. 2007;27(2):190-202.
24.   Weisel FJ, Mullett SJ, Elsner RA, Menk AV, Trivedi N, Luo W, et al. Germinal center B cells selectively oxidize fatty acids for energy while conducting minimal glycolysis. Nature immunology. 2020;21(3):331-42.
25.   Yan J, Horng T. Lipid Metabolism in Regulation of Macrophage Functions. Trends in cell biology. 2020;30(12):979-89.
26.   Moreno-Altamirano MMB, Kolstoe SE, Sanchez-Garcia FJ. Virus Control of Cell Metabolism for Replication and Evasion of Host Immune Responses. Frontiers in cellular and infection microbiology. 2019;9:95.
27.   Heaton NS, Randall G. Multifaceted roles for lipids in viral infection. Trends in microbiology. 2011;19(7):368-75.
28.   Thaker SK, Ch'ng J, Christofk HR. Viral hijacking of cellular metabolism. BMC biology. 2019;17(1):59.
29.   Vastag L, Koyuncu E, Grady SL, Shenk TE, Rabinowitz JD. Divergent effects of human cytomegalovirus and herpes simplex virus-1 on cellular metabolism. PLoS pathogens. 2011;7(7):e1002124.
30.   Thai M, Thaker SK, Feng J, Du Y, Hu H, Ting Wu T, et al. MYC-induced reprogramming of glutamine catabolism supports optimal virus replication. Nature communications. 2015;6:8873.
31.   Yu Y, Clippinger AJ, Alwine JC. Viral effects on metabolism: changes in glucose and glutamine utilization during human cytomegalovirus infection. Trends in microbiology. 2011;19(7):360-7.
32.   Munger J, Bennett BD, Parikh A, Feng XJ, McArdle J, Rabitz HA, et al. Systems-level metabolic flux profiling identifies fatty acid synthesis as a target for antiviral therapy. Nature biotechnology. 2008;26(10):1179-86.
33.   Lercher A, Bhattacharya A, Popa AM, Caldera M, Schlapansky MF, Baazim H, et al. Type I Interferon Signaling Disrupts the Hepatic Urea Cycle and Alters Systemic Metabolism to Suppress T Cell Function. Immunity. 2019;51(6):1074-87 e9.
34.   Kosack L, Gawish R, Lercher A, Vilagos B, Hladik A, Lakovits K, et al. The lipid-sensor TREM2 aggravates disease in a model of LCMV-induced hepatitis. Scientific reports. 2017;7(1):11289.
35.   Eckel RH, Grundy SM, Zimmet PZ. The metabolic syndrome. Lancet. 2005;365(9468):1415-28.
36.   Stoeckle M, Kaech C, Trampuz A, Zimmerli W. The role of diabetes mellitus in patients with bloodstream infections. Swiss medical weekly. 2008;138(35-36):512-9.
37.   Rao Kondapally Seshasai S, Kaptoge S, Thompson A, Di Angelantonio E, Gao P, Sarwar N, et al. Diabetes mellitus, fasting glucose, and risk of cause-specific death. The New England journal of medicine. 2011;364(9):829-41.
38.   Muller LM, Gorter KJ, Hak E, Goudzwaard WL, Schellevis FG, Hoepelman AI, et al. Increased risk of common infections in patients with type 1 and type 2 diabetes mellitus. Clinical infectious diseases : an official publication of the Infectious Diseases Society of America. 2005;41(3):281-8.
39.   Gupta S, Koirala J, Khardori R, Khardori N. Infections in diabetes mellitus and hyperglycemia. Infectious disease clinics of North America. 2007;21(3):617-38, vii.

40.   Jeon CY, Murray MB. Diabetes mellitus increases the risk of active tuberculosis: a systematic review of 13 observational studies. PLoS medicine. 2008;5(7):e152.

41.   Guo W, Li M, Dong Y, Zhou H, Zhang Z, Tian C, et al. Diabetes is a risk factor for the progression and prognosis of COVID-19. Diabetes/metabolism research and reviews. 2020;36(7):e3319.

42.   Yang J, Zheng Y, Gou X, Pu K, Chen Z, Guo Q, et al. Prevalence of comorbities and its effects in patients infected with SARS-CoV-2: a systematic review and meta-analysis. International journal of infectious diseases : IJID : official publication of the International Society for Infectious Diseases. 2020;94:91-5.

43.   Wensveen FM, Sestan M, Turk Wensveen T, Polic B. Blood glucose regulation in context of infection. Vitamins and hormones. 2021;117:253-318.

44.   Wensveen FM, Jelencic V, Valentic S, Sestan M, Wensveen TT, Theurich S, et al. NK cells link obesity-induced adipose stress to inflammation and insulin resistance. Nature immunology. 2015;16(4):376-85.

45.   Saisho Y. Importance of Beta Cell Function for the Treatment of Type 2 Diabetes. Journal of clinical medicine. 2014;3(3):923-43.

46.   Bandaru P, Shankar A. Association between plasma leptin levels and diabetes mellitus. Metabolic syndrome and related disorders. 2011;9(1):19-23.

47.   Kornum JB, Thomsen RW, Riis A, Lervang HH, Schonheyder HC, Sorensen HT. Diabetes, glycemic control, and risk of hospitalization with pneumonia: a population-based case-control study. Diabetes care. 2008;31(8):1541-5.

48.   Simonsen JR, Harjutsalo V, Jarvinen A, Kirveskari J, Forsblom C, Groop PH, et al. Bacterial infections in patients with type 1 diabetes: a 14-year follow-up study. BMJ open diabetes research & care. 2015;3(1):e000067.

49.   Khodakhah F, Tahamtan A, Marzban M, Shadab A, Tavakoli-Yaraki M, Hashemi SM, et al. Hyperglycemia results in decreased immune cell infiltration and increased viral load in the lung in a mouse model of RSV infection. Cytokine. 2021;143:155539.

50.   Ayelign B, Negash M, Genetu M, Wondmagegn T, Shibabaw T. Immunological Impacts of Diabetes on the Susceptibility of Mycobacterium tuberculosis. Journal of immunology research. 2019;2019:6196532.

51.   Wensveen FM, Valentic S, Sestan M, Turk Wensveen T, Polic B. The "Big Bang" in obese fat: Events initiating obesity-induced adipose tissue inflammation. European journal of immunology. 2015;45(9):2446-56.

52.   Esser N, Legrand-Poels S, Piette J, Scheen AJ, Paquot N. Inflammation as a link between obesity, metabolic syndrome and type 2 diabetes. Diabetes research and clinical practice. 2014;105(2):141-50.

53.   Association AD. Comprehensive Medical Evaluation and Assessment of Comorbidities: Standards of Medical Care in Diabetes-2020. Diabetes care. 2020;43:S37-S47.

54.   Tabak AG, Herder C, Rathmann W, Brunner EJ, Kivimaki M. Prediabetes: a high-risk state for diabetes development. Lancet. 2012;379(9833):2279-90.

55.   Montefusco L, Ben Nasr M, D'Addio F, Loretelli C, Rossi A, Pastore I, et al. Acute and long-term disruption of glycometabolic control after SARS-CoV-2 infection. Nature metabolism. 2021;3(6):774-85.

56.   Tsai S, Clemente-Casares X, Zhou AC, Lei H, Ahn JJ, Chan YT, et al. Insulin Receptor-Mediated Stimulation Boosts T Cell Immunity during Inflammation and Infection. Cell metabolism. 2018;28(6):922-34 e4.

57.   Cantrell CB MS. Ketone metabolism. Biochemistry. 2022.

58.   Azoulay E, Chevret S, Didier J, Barboteu M, Bornstain C, Darmon M, et al. Infection as a trigger of diabetic ketoacidosis in intensive care-unit patients. Clinical infectious diseases : an official publication of the Infectious Diseases Society of America. 2001;32(1):30-5.

59.   Umpierrez GE, Kitabchi AE. Diabetic ketoacidosis: risk factors and management strategies. Treatments in endocrinology. 2003;2(2):95-108.

60.   Desruisseaux MS, Nagajyothi, Trujillo ME, Tanowitz HB, Scherer PE. Adipocyte, adipose tissue, and infectious disease. Infection and immunity. 2007;75(3):1066-78.

61.   Choe SS, Huh JY, Hwang IJ, Kim JI, Kim JB. Adipose Tissue Remodeling: Its Role in Energy Metabolism and Metabolic Disorders. Frontiers in endocrinology. 2016;7:30.

62.   Lolmede K, Duffaut C, Zakaroff-Girard A, Bouloumie A. Immune cells in adipose tissue: key players in metabolic disorders. Diabetes & metabolism. 2011;37(4):283-90.

63.   Lu J, Zhao J, Meng H, Zhang X. Adipose Tissue-Resident Immune Cells in Obesity and Type 2 Diabetes. Frontiers in immunology. 2019;10:1173.

64.   Ayres JS. Immunometabolism of infections. Nature reviews Immunology. 2020;20(2):79-80.

65.   Jager J, Gremeaux T, Cormont M, Le Marchand-Brustel Y, Tanti JF. Interleukin-1beta-induced insulin resistance in adipocytes through down-regulation of insulin receptor substrate-1 expression. Endocrinology. 2007;148(1):241-51.

66.   Grunfeld C, Zhao C, Fuller J, Pollack A, Moser A, Friedman J, et al. Endotoxin and cytokines induce expression of leptin, the ob gene product, in hamsters. The Journal of clinical investigation. 1996;97(9):2152-7.

67.   Wensveen FM, Sestan M, Turk Wensveen T, Polic B. 'Beauty and the beast' in infection: How immune-endocrine interactions regulate systemic metabolism in the context of infection. European journal of immunology. 2019;49(7):982-95.

68.   Wentworth JM, Zhang JG, Bandala-Sanchez E, Naselli G, Liu R, Ritchie M, et al. Interferon-gamma released from omental adipose tissue of insulin-resistant humans alters adipocyte phenotype and impairs response to insulin and adiponectin release. International journal of obesity. 2017;41(12):1782-9.

69.   Agarwal N, Balasubramanyam A. Viral mechanisms of adipose dysfunction: lessons from HIV-1 Vpr. Adipocyte. 2015;4(1):55-9.

70.   Damouche A, Lazure T, Avettand-Fenoel V, Huot N, Dejucq-Rainsford N, Satie AP, et al. Adipose Tissue Is a Neglected Viral Reservoir and an Inflammatory Site during Chronic HIV and SIV Infection. PLoS pathogens. 2015;11(9):e1005153.

71.   Baazim H, Schweiger M, Moschinger M, Xu H, Scherer T, Popa A, et al. CD8(+) T cells induce cachexia during chronic viral infection. Nature immunology. 2019;20(6):701-10.

72.   Gebhardt T, Wakim LM, Eidsmo L, Reading PC, Heath WR, Carbone FR. Memory T cells in nonlymphoid tissue that provide enhanced local immunity during infection with herpes simplex virus. Nature immunology. 2009;10(5):524-30.

73.   Hammarlund E, Lewis MW, Hansen SG, Strelow LI, Nelson JA, Sexton GJ, et al. Duration of antiviral immunity after smallpox vaccination. Nature medicine. 2003;9(9):1131-7.

74.   Zebisch K, Voigt V, Wabitsch M, Brandsch M. Protocol for effective differentiation of 3T3-L1 cells to adipocytes. Analytical biochemistry. 2012;425(1):88-90.

75.   Kavazovic I, Han H, Balzaretti G, Slinger E, Lemmermann NAW, Ten Brinke A, et al. Eomes broadens the scope of CD8 T-cell memory by inhibiting apoptosis in cells of low affinity. PLoS biology. 2020;18(3):e3000648.

76.   Sarafian MH, Gaudin M, Lewis MR, Martin FP, Holmes E, Nicholson JK, et al. Objective set of criteria for optimization of sample preparation procedures for ultra-high throughput untargeted blood plasma lipid profiling by ultra performance liquid chromatography-mass spectrometry. Analytical chemistry. 2014;86(12):5766-74.

77.   Li M, Fu W, Li XA. Differential fatty acid profile in adipose and non-adipose tissues in obese mice. International journal of clinical and experimental medicine. 2010;3(4):303-7.

78.   Hodson L, Skeaff CM, Fielding BA. Fatty acid composition of adipose tissue and blood in humans and its use as a biomarker of dietary intake. Progress in lipid research. 2008;47(5):348-80.

79.   Zhang Z, Shu G, Zhu X, Guo J, Cai H, Wang S, et al. Effect of diacylglycerol acyltransferase 2 overexpression in 3T3-L1 is associated to an increase in mono-unsaturated fatty acid accumulation. Journal of animal science and biotechnology. 2014;5(1):29.

80.   Mead JR, Irvine SA, Ramji DP. Lipoprotein lipase: structure, function, regulation, and role in disease. Journal of molecular medicine. 2002;80(12):753-69.

81.   Niu H, Cattoretti G, Dalla-Favera R. BCL6 controls the expression of the B7-1/CD80 costimulatory receptor in germinal center B cells. The Journal of experimental medicine. 2003;198(2):211-21.

82.   Rose KL, Pin CL, Wang R, Fraser DD. Combined insulin and bicarbonate therapy elicits cerebral edema in a juvenile mouse model of diabetic ketoacidosis. Pediatric research. 2007;61(3):301-6.

83.   Kawai M, Rosen CJ. PPARgamma: a circadian transcription factor in adipogenesis and osteogenesis. Nature reviews Endocrinology. 2010;6(11):629-36.

84.   Chang CH, Curtis JD, Maggi LB, Jr., Faubert B, Villarino AV, O'Sullivan D, et al. Posttranscriptional control of T cell effector function by aerobic glycolysis. Cell. 2013;153(6):1239-51.

85.   Jacobs SR, Herman CE, Maciver NJ, Wofford JA, Wieman HL, Hammen JJ, et al. Glucose uptake is limiting in T cell activation and requires CD28-mediated Akt-dependent and independent pathways. Journal of immunology. 2008;180(7):4476-86.

86.   Araki K, Ahmed R. AMPK: a metabolic switch for CD8+ T-cell memory. European journal of immunology. 2013;43(4):878-81.

87.   Araki K, Turner AP, Shaffer VO, Gangappa S, Keller SA, Bachmann MF, et al. mTOR regulates memory CD8 T-cell differentiation. Nature. 2009;460(7251):108-12.

88.   Raud B, McGuire PJ, Jones RG, Sparwasser T, Berod L. Fatty acid metabolism in CD8(+) T cell memory: Challenging current concepts. Immunological reviews. 2018;283(1):213-31.

89.   Krapic M, Kavazovic I, Wensveen FM. Immunological Mechanisms of Sickness Behavior in Viral Infection. Viruses. 2021;13(11).

90.   Laine PS, Schwartz EA, Wang Y, Zhang WY, Karnik SK, Musi N, et al. Palmitic acid induces IP-10 expression in human macrophages via NF-kappaB activation. Biochemical and biophysical research communications. 2007;358(1):150-5.

91.   Zhou X, Zhu X, Zeng H. Fatty acid metabolism in adaptive immunity. The FEBS journal. 2023;290(3):584-99.

92.   Ramon S, Bancos S, Thatcher TH, Murant TI, Moshkani S, Sahler JM, et al. Peroxisome proliferator-activated receptor gamma B cell-specific-deficient mice have an impaired antibody response. Journal of immunology. 2012;189(10):4740-7.

93.   Grygiel-Gorniak B. Peroxisome proliferator-activated receptors and their ligands: nutritional and clinical implications--a review. Nutrition journal. 2014;13:17.

94.   Man K, Kallies A, Vasanthakumar A. Resident and migratory adipose immune cells control systemic metabolism and thermogenesis. Cellular & molecular immunology. 2022;19(3):421-31.

95.   Bourgeois C, Gorwood J, Barrail-Tran A, Lagathu C, Capeau J, Desjardins D, et al. Specific Biological Features of Adipose Tissue, and Their Impact on HIV Persistence. Frontiers in microbiology. 2019;10:2837.

96.   Wani K, AlHarthi H, Alghamdi A, Sabico S, Al-Daghri NM. Role of NLRP3 Inflammasome Activation in Obesity-Mediated Metabolic Disorders. International journal of environmental research and public health. 2021;18(2).

97.   Richard AJ, Stephens JM. The role of JAK-STAT signaling in adipose tissue function. Biochimica et biophysica acta. 2014;1842(3):431-9.

98.   Waite KJ, Floyd ZE, Arbour-Reily P, Stephens JM. Interferon-gamma-induced regulation of peroxisome proliferator-activated receptor gamma and STATs in adipocytes. The Journal of biological chemistry. 2001;276(10):7062-8.

99.   Hogan JC, Stephens JM. The identification and characterization of a STAT 1 binding site in the PPARgamma2 promoter. Biochemical and biophysical research communications. 2001;287(2):484-92.

100.   McGillicuddy FC, Chiquoine EH, Hinkle CC, Kim RJ, Shah R, Roche HM, et al. Interferon gamma attenuates insulin signaling, lipid storage, and differentiation in human adipocytes via activation of the JAK/STAT pathway. The Journal of biological chemistry. 2009;284(46):31936-44.

101.   Waters LR, Ahsan FM, Wolf DM, Shirihai O, Teitell MA. Initial B Cell Activation Induces Metabolic Reprogramming and Mitochondrial Remodeling. iScience. 2018;5:99-109.

102.   Santa-Maria C, Lopez-Enriquez S, Montserrat-de la Paz S, Geniz I, Reyes-Quiroz ME, Moreno M, et al. Update on Anti-Inflammatory Molecular Mechanisms Induced by Oleic Acid. Nutrients. 2023;15(1).

103.   Gorjao R, Cury-Boaventura MF, de Lima TM, Curi R. Regulation of human lymphocyte proliferation by fatty acids. Cell biochemistry and function. 2007;25(3):305-15.

104.   Ioan-Facsinay A, Kwekkeboom JC, Westhoff S, Giera M, Rombouts Y, van Harmelen V, et al. Adipocyte-derived lipids modulate CD4+ T-cell function. European journal of immunology. 2013;43(6):1578-87.

105.   Feng J, Liu X, Ni X, Qi H. External signals regulate germinal center fate-determining transcription factors in the A20 lymphoma cell line. Molecular immunology. 2018;93:79-86.

106.   Slavik JM, Hutchcroft JE, Bierer BE. CD28/CTLA-4 and CD80/CD86 families: signaling and function. Immunologic research. 1999;19(1):1-24.

107.   Hong S, Zhang Z, Liu H, Tian M, Zhu X, Zhang Z, et al. B Cells Are the Dominant Antigen-Presenting Cells that Activate Naive CD4(+) T Cells upon Immunization with a Virus-Derived Nanoparticle Antigen. Immunity. 2018;49(4):695-708 e4.

108.   Shaikh SR, Mitchell D, Carroll E, Li M, Schneck J, Edidin M. Differential effects of a saturated and a monounsaturated fatty acid on MHC class I antigen presentation. Scandinavian journal of immunology. 2008;68(1):30-42.

109.   Demetrius L. Of mice and men. When it comes to studying ageing and the means to slow it down, mice are not just small humans. EMBO reports. 2005;6 Spec No(Suppl 1):S39-44.

110.   Stevens JS, Bogun MM, McMahon DJ, Zucker J, Kurlansky P, Mohan S, et al. Diabetic ketoacidosis and mortality in COVID-19 infection. Diabetes & metabolism. 2021;47(6):101267.

LIST OF FIGURES

LIST OF TABLES

ABBREVATIONS LIST

ACC	- Acetyl-CoA carboxylase
ACTH	- Adrenocorticotropic hormone
ALX	- Alloxan
AMPK	- AMP-activated protein kinase
ATP	- Adenosine triphosphate
BAC	- Bacterial artificial chromosome
BSA	- Bovine serum albumin
CNS	- Central nervous system
DGAT2	- Diacylglycerol O-acyltransferase 2
DKA	- Diabetic ketoacidosis
DMEM	- Dulbecco's modified eagle medium
EP3R	- The prostaglandin E receptor 3
FACS	- Fluorescence-activated cell sorting
FAS	- Fatty acid synthase
FCCP	- Carbonyl cyanide-4 (trifluoromethoxy) phenylhydrazone
FCS	- Fetal Calf Serum
FFA	- Free fatty acids
GLUT4	- Glucose transporter type 4
hCMV	- Human cytomegalovirus
HCV	- Hepatitis C virus
HFD	- High fat diet
HIV	- Human immunodeficiency virus
HSV-1	- Herpes simplex virus-1
IFNs	- Interferons
IFU	- Infectious focus units
ILs	- Interleukins
i.p.	- Intraperitoneally

IR   - Insulin resistance

i.v.   - Intravenously

IVC   - Individually ventilated caging

JAK/STAT   - Janus kinase/signal transducer and activator of transcription

LC-MS   - Liquid chromatography-mass spectrometry

LCMV   - Lymphocytic choriomeningitis virus

LPL   - Lipoprotein lipase

MACS   - Magnetic-activated cell sorting

mCMV   - Murine cytomegalovirus

mTOR   - Mammalian target of rapamycin

N4   - SIINFEKL; ovalbumin

NCR1   - NK cell–activating receptor 1

NK   - Natural killer

NLRP3   - NLR family pyrin domain containing 3

n.s.   - Not significant

OA   - Oleic acid

OCR   - Oxygen consumption rate

PCR   - Polymerase Chain Reaction

PFU   - Plaque-forming unit

PGE2   - Prostaglandin E2

PPARγ   - Peroxisome proliferator-activated receptor-gamma

RPMI   - Roswell park memorial institute medium

RSV   - Respiratory Syncytial virus

RT-PCR   - Reverse transcription polymerase chain reaction

RU   - Relative unit

SARS-CoV-2 - Severe acute respiratory syndrome coronavirus 2

s.e.m.   - Standard error of the mean

SIV   - Simian immunodeficiency virus

STZ   - Streptozotocin

SVF   - Stromal vascular fraction

TNF   - Tumor necrosis factor

T2D   - Type 2 diabetes

VAT   - Visceral adipose tissue

WT   - Wild type

CURRICULUM VITAE

PERSONAL INFORMATION

Name	MIA KRAPIĆ
Address	Drenovski put 3, 51000 Rijeka, Croatia
Telephone	+385 998204754
E-mail	mia.krapic@medri.uniri.hr

Date of birth	08/02/1995

WORK EXPERIENCE

• *March, 2019 - /* • *Faculty of Medicine, Rijeka (Croatia) – Department of histology and embryology*	Assistant, PhD student

EDUCATION AND TRAINING

• *June 2020 - /* • *Faculty of Medicine, Rijeka (Croatia)*	Postgraduate study program "Biomedicine"
• *2016 – 2018* • *Department of biotechnology, Rijeka (Croatia)*	Graduate university program "Biotechnology in Medicine" • Master's thesis „Size-exclusion chromatography-based isolation of extracellular vesicles from cerebrospinal fluid of patients with severe traumatic brain injury" • Faculty of Medicine, Rijeka (Croatia) – Department of physiology, immunology and pathophysiology • Mentor: Assist. Prof. Kristina Grabušić
• *2013 – 2016* • *Department of biotechnology, Rijeka (Croatia)*	Undergraduate university program "Biotechnology and Drug Research"
• *2009-2013* • *Gimnazija Andrije Mohorovičića Rijeka*	High school – gymnasium

CONGRESSES AND MEETINGS

• FEBS Immunology Summer School, Hvar, 2019 (active participant - poster presentation)

Abstract title: Insulin receptor-deficiency on CD8 T cells does not affect memory responses
Authors: Inga Kavazović, Mia Krapić, Felix M. Wensveen

• The annual meeting of the Croatian society for immunology, Rovinj, 2019 (active participant - poster presentation)
Abstract title: Insulin receptor-deficiency on CD8 T cells does not affect memory responses
Authors: Inga Kavazović, Mia Krapić, Felix M. Wensveen

• The annual meeting of the Croatian society for immunology, 2020 (active participant - oral presentation)
Abstract title: IFN-γ produced in infection down-regulates PPAR-γ and changes adipose tissue biology
Authors: Mia Krapić, Felix M. Wensveen

• Keystone symposia eSymposia meeting Metabolic decisions in development and disease, 2021 (active participant - poster presentation)
Abstract title: IFN-γ produced in infection down-regulates PPAR-γ to modulate adipose tissue biology
Authors: Mia Krapić, Inga Kavazović, Tamara Turk Wensveen, Felix M. Wensveen

• 6th European congress of immunology, 2021 (active participant - poster presentation)
Abstract title: IFN-γ produced in infection down-regulates PPAR-γ to modulate adipose tissue biology
Authors: Mia Krapić, Inga Kavazović, Tamara Turk Wensveen, Felix M. Wensveen

• The annual meeting of the Croatian society for immunology, Trogir, 2021 (active participant – poster presentation)
Abstract title: IFN-γ produced in infection down-regulates PPAR-γ to modulate adipose tissue biology
Authors: Mia Krapić, Inga Kavazović, Tamara Turk Wensveen, Felix M. Wensveen

• 15th ENII EFIS EJI summer school on advanced immunology, Alghero, Sardinia, 2022 (active participant – oral and poster presentation)
Abstract title: IFN-γ produced in infection down-regulates PPAR-γ to modulate adipose tissue biology and systemic metabolism
Authors: Mia Krapić, Inga Kavazović, Tamara Turk Wensveen, Felix M. Wensveen

• The annual meeting of the Croatian society for immunology, Sv. Martin na Muri 2022 (active participant – poster presentation)
Abstract title: NK cell derived IFN-γ causes free fatty acid release by adipocytes to promote B cell responses during viral infection
Authors: Mia Krapić, Inga Kavazović, Tamara Turk Wensveen, Felix M. Wensveen

• First place award in the National student Start-up competition, Zagreb, 2016
• Finished Undergraduate university program "with great honor" - magna cum laude

• Approved financial resources for the project "Characterisation of EV in patients with TBI" by the Student council of the University of Rijeka, 2017
• Third place award for poster presentation at the International Student Congress (ISC) of the Medical University of Graz, 2018
• Finished Graduate university program "with great honor" - magna cum laude
• EFIS best poster award at the 6th European congress of immunology, 2021

• American summer school: pathophysiology of public health issues and diseases, Rijeka, 2017
• FEBS Immunology Summer School, Hvar, 2019
• 15th ENII EFIS EJI summer school on advanced immunology, Alghero, Sardinia, 2022

EFIS short-term fellowship, 2022

• August 8th – September 16th 2022 Faculty of medicine, Technical university Munich, laboratory of Prof. dr. Marc Schmidt-Supprian

Martens, Anne W. J.; Kavazović, Inga; **Krapić, Mia**; Pack, Su Min; Arens, Ramon; Jongejan, Aldo; Moerland, Perry D.; Eldering, Eric; van der Windt, Gerritje J. W.; Wensveen, Felix M. et al.
Chronic lymphocytic leukemia presence impairs antigen-specific CD8+ T-cell responses through epigenetic reprogramming towards short-lived effectors. Leukemia, 2023 (IF:11.5)

Kavazović, Inga; **Krapić, Mia**; Beumer-Chuwonpad, Ammarina; Polić, Bojan; Turk Wensveen, Tamara; Lemmermann, Niels A.; van Gisbergen, Klaas P.J.M.; Wensveen, Felix M.
Hyperglycemia and Not Hyperinsulinemia Mediates Diabetes-Induced Memory CD8 T-Cell Dysfunction. Diabetes, 2022 (IF:9.3)

Krapić, Mia; Kavazović, Inga; Wensveen, Felix M.
Immunological Mechanisms of Sickness Behavior in Viral Infection. Viruses 2021 (IF:5.8)